METEOROLOGICAL RESPONSE TO CO_2 SEQUESTRATION AND STORAGE IN ANTARCTICA

by

Andrea Orton

A Dissertation

Submitted to the Faculty of Purdue University

In Partial Fulfillment of the Requirements for the degree of

Doctor of Philosophy

Earth, Atmospheric, and Planetary Sciences

West Lafayette, Indiana

May 2020

THE PURDUE UNIVERSITY GRADUATE SCHOOL
STATEMENT OF COMMITTEE APPROVAL

Dr. Ernest Agee, Co-Chair

Earth, Atmospheric, and Planetary Sciences

Dr. Michael Baldwin, Co-Chair

Earth, Atmospheric, and Planetary Sciences

Dr. Dan Chavas

Earth, Atmospheric, and Planetary Sciences

Dr. Bob Jacko

Civil Engineering

Dr. Rich Neale

National Center for Atmospheric Research

Approved by:

Dr. Daniel Cziczo

This dissertation is dedicated to my parents and brother for their endless patience and open ears for which they let me use to practice all my seminars. This is also dedicated to my advisors, Ernest Agee and Michael Baldwin, for their supportive guidance and mentorship that will stay with me the rest of my career.

ACKNOWLEDGMENTS

To start the acknowledgements, my advisors Ernest Agee and Michael Baldwin have been the main source of support for this entire PhD research project. Their insight and suggestions to get around research walls helped to get the research to this point.

Rich Neale, my committee member and sponsor at NCAR in November 2018, jumpstarted all the CESM simulations discussed in this research. There is no way we would have started any of this work, let alone complete it, without his help. Further, all simulations were ran on Cheyenne which served as a very accessible and efficient computing tool for all research conducted.

My lab mate, Gillian Ferguson, helped gather CO_2 data for this analysis which helped compare observations to model output.

Finally, Dr. Jacko and Dr. Chavas serving as my committee members and professors have given me knowledge that has deepened my critical thinking to become a better researcher. Their willingness to help and serve on my committee has been invaluable.

TABLE OF CONTENTS

LIST OF TABLES

LIST OF FIGURES

ABSTRACT

Increasing CO_2 concentrations in the Earth's atmosphere have led to global warming with climate change effects. Future RCP scenarios per the IPCC suggest that local solutions to limit emissions are necessary but may not suffice to combat the anthropogenic CO_2 problem. Climate intervention has been given increasing consideration. A climate intervention approach of removing CO_2 from the atmosphere through dry ice deposition and storage in Antarctica is considered. While the technology needs continued development, understanding the meteorological response to significant carbon dioxide removal (CDR) in Antarctica takes precedence. Various Antarctica CDR scenarios are simulated through the fully-coupled general circulation model CESM 2.1.1. Modern simulations (15 years) with prognostic CO_2 include 1) anthropogenic emissions (control), 2) no emissions, 3) emissions with ~4.5 ppmv sequestration annually (half sequestration), and 4) emissions with ~9 ppmv sequestration annually (full sequestration). Full sequestration attempts to remove enough CO_2 to achieve pre-industrial concentration by the end of the simulation. Experiments 1) and 3) were continued until mid-21st century (50 years total) with SSP1-2.6 conditions and emissions to examine the CDR impact on the atmosphere under the Paris Treaty Agreement scenario (which limits Earth's warming to 1.5^{o}C-2^{o}C above pre-industrial values).

Modern simulations show sequestration scenarios have more of an impact on 2m-air temperature and little effect on precipitation patterns in 15 years. SSP1-2.6 simulations show that an additional 1^{o}C of warming can be inhibited by continuing sequestration and limiting emissions. Further, sequestration shows counteraction to warming in many of the locations that are predicted to warm per the RCP 2.6 scenario in the IPCC (2013), as well as counteraction to the predicted IPCC precipitation changes. These results are obtained from one simulation of each experiment, and it is recognized that ensemble runs in line with IPCC predictions are necessary to examine all possible predictions to CDR. Future considerations include sea level rise, carbon cycle response, convective parameters, and relocation of sequestration.

CHAPTER 1. INTRODUCTION & BACKGROUND

Earth's general atmospheric circulation is driven by the equator-pole temperature gradient induced from solar radiation distribution and the Earth's tilted rotation. By transporting warm air poleward and cold air to the tropics, the atmospheric circulation is essential for balancing out the distribution of heat in both hemispheres. Since every location on Earth heats up and cools uniquely due to its surface and atmospheric conditions, the resulting average weather patterns (or climate) vary around the world. Different types of clouds and surfaces absorb, transmit, and/or reflect solar and terrestrial radiation influencing the characteristics of overlying air masses. The atmosphere is made of different gases that influence Earth's radiation budget, some of which have a role in the greenhouse effect by selectively absorbing and emitting solar and infrared radiation. Without the infrared radiative effects of greenhouse gases, the Earth would be much cooler. The two primary greenhouse gases are water vapor and carbon dioxide with their strong absorption bands of terrestrial radiation. Warming associated with increasing CO_2 also produces additional potential greenhouse effect due to the associated increases of atmospheric water vapor.

Past natural variations in climate (in particular the Milankovitch cycles associated with the Earth's orbital parameters) have resulted in 100,000 year epochs of continental glaciations. Evidence of the greenhouse effect in past climate variations can be found in ice core analysis that shows carbon dioxide concentrations never exceeded 300ppmv in the past 900,000 years. These higher CO_2 concentrations were associated with interglacial periods and the lower concentrations were associated with continental glaciations (where CO_2 was held in continental ice storage as well as in colder oceans). Presently, global atmospheric carbon dioxide concentration exceeds 400ppmv, well above the representative pre-industrial concentration value of 280 ppmv. This steep increase in atmospheric CO_2 for the past century is considered to be the primary cause of global warming resulting in $\sim 1^{o}C$ temperature increase and associated effects such as the melting of the Arctic and sea ice, partial melting of the Greenland ice cap, and sea level rise (IPCC, 2013). Current global warming is occurring on a much shorter time scale than the ice core record, prompting the scientific community to investigate and provide evidence of anthropogenic climate change and suggestions for mitigation.

The IPCC AR5 WGI has projected future climates based upon CO_2 concentrations from possible anthropogenic emissions scenarios with Representative Concentration Pathways (RCPs).

The four RCPs (2.6 Wm^{-2}, 4.5 Wm^{-2}, 6.0 Wm^{-2}, and 8.5 Wm^{-2}) are representative of the radiative forcing values by the end of the 21st century relative to pre-industrial values. Climate modeling of all RCPs has predicted a range of 0.3-4.8^{o}C increase in global mean temperature and a corresponding range of 0.26-0.82 meters increase in global mean sea level (IPCC, 2013). Such potential realities will challenge society into adapting to these climate change effects. Additional future climate projections from the IPCC have affirmed serious consideration of alternative energy infrastructure modifications to reduce CO_2 emissions such as wind energy, biofuels, solar energy, and carbon capture and storage (CCS). In the international relations arena, the Paris Agreement is an effort for international collaboration to limit Earth's warming to only 2^{o}C above pre-industrial temperatures. Since carbon dioxide is a stable gas that can remain in the atmosphere for hundreds of years, reducing emissions may not suffice considering the predicted long-term impacts of anthropogenic climate change (with CO_2 warming effects already built into the system without CCS). For this reason, other strategies are being considered on the global scale.

1.1 Climate Intervention (Geoengineering)

Global scale intervention to modify the Earth's climate system to reverse the effects of global warming, known as climate intervention, has been given increasing consideration as a possible solution along with renewable energy to global warming. The National Academy of Sciences has assembled a committee to research climate intervention proposals consisting of albedo modification and carbon dioxide removal (National Research Council, 2015).

1.1.1 Albedo Modification

Albedo modification methods of stratospheric aerosol injection and marine cloud brightening seek to reflect a portion of incoming solar radiation back to space to counteract anthropogenic increases in temperature and associated climate change. There have been studies done on stratospheric aerosol injection (for example Tilmes et al., 2016) that have provided a thorough path for climate intervention research for examining impacts and caveats. An overview of the Geoengineering Large Ensemble (GLENS) project described in the Tilmes et al., 2018 BAMS article describes the approaches taken in research to understand the effect of stratospheric

aerosol engineering while meeting specific climate goals. The author used the Community Earth System Model version 1 (CESM) with the Whole Atmosphere Community Climate Model (WACCM) as the atmosphere component. This atmospheric component is coupled to the land, sea ice, and ocean. In the studies, four locations served as the injection sites at 30^{o}N, 15^{o}N, 15^{o}S, and 30^{o}S at a height ~5 km above the troposphere. Previous studies have shown that there is a potential for uneven cooling between the two hemispheres that can lead to shifts in precipitation patterns (Haywood et al., 2013 and Jones et al. 2017). These locations chosen for injection are enough to modify the stratosphere aerosol distribution to maintain the global mean surface temperature, the interhemispheric temperature, and equator-pole temperature gradient (Kravitz et al., 2017). The study used a 20 member geoengineering large ensemble focusing on the RCP 8.5 scenario. Results show that the lower tropical stratospheric temperatures increase ~5^{o}C after 20 years and 10^{o}C after 80 years. These changes can have important implications for evolution of stratospheric column ozone that affects the amount of short wave radiation reaching the surface. For global surface temperature, the application of stratospheric aerosol injection prevents significant temperature change in comparison to RCP 8.5 without geoengineering. (Tilmes et al., 2018).

Though albedo modification can create immediate cooling, it does not solve the cause of anthropogenic climate change from increasing emissions of greenhouse gases. Further, there could be global risks associated with albedo modification if abruptly terminated with future emissions scenarios per the IPCC (National Research Council, 2015). The stratospheric temperature changes outlined in the Tilmes et al. (2018) study discusses the potential modification to the QBO which can affect tropospheric winds and temperatures.

1.1.2 Carbon Dioxide Removal (CDR)

Carbon dioxide removal (CDR) methods such as land management strategies, ocean iron fertilization, accelerated weathering, bioenergy with carbon capture and storage (CCS), and direct air capture and sequestration focus on removal of carbon dioxide from the atmosphere. As opposed to albedo modification, CDR technologies a) directly address anthropogenic climate change, b) do not produce known significant risks if terminated abruptly, c) can have a modest impact on climate within decades, d) are potentially expensive, and e) may require reduction of industrial emissions to have a substantial impact on climate. (National Research Council, 2015).

There are four companies creating CO_2 "scrubbers" that use chemical processes to extract the CO_2 from the air. Carbon Engineering, Global Thermostat, Climeworks, and a group at Arizona State University are working on developing these plants to scale to sequester on the global scale. Costs of removal per ton of CO_2 range from $100-$600. There has yet to be proof of a necessary operational cost of <$100 per ton of CO_2. (Kramer, 2020). In terms of storage, the total global geological storage capacity has an estimated range of 550 GtC-1900 GtC (Tavoni and Socolow, 2013).

Since CDR has been acknowledged as the technology that poses the least amount of risk, it is potentially the more ideal solution to pursue for mitigating anthropogenic climate change. In reference to cost and CDR's impact on climate, it is worth evaluating the different proposals and associated choice of method. Different methods use different amounts of energy, but energy requirements have the potential to be minimized if installation is at an appropriate geographical location with supporting environmental variables for large amounts of sequestration and storage. Such a human-made large-scale CO_2 sink would impact global redistribution of the CO_2 and associated radiative forcing. Response of meteorological phenomena could be influenced by this CO_2 radiative forcing redistribution, especially if the sequestration is occurring at the coldest, most southern continent on Earth that provides an environment for atmospheric CO_2 deposition and storage.

1.1.2.1 CO_2 Sequestration and Storage in Antarctica

Agee et al. (2013) (to be referred to as AOR) proposes using closed-loop liquid nitrogen refrigeration facilities to freeze out atmospheric CO_2 at surface pressure in Antarctica and storing the dry ice in insulated landfills within the Antarctic ice. Atmospheric constituents such as N_2, O_2, and Ar remain in their gas phases at the CO_2 deposition temperature of 133K in Antarctica (resulting in CO_2 snow). The AOR plan places wind farms placed on the coast of Antarctica would that provide the energy to the 446 sequestration plants to remove 1 billion tons of carbon annually (~0.5ppmv of CO_2). Antarctica is an ideal location for such a direct air capture process due to the resources readily available: dry and cold conditions, abundance of wind energy from the katabatic winds, vast area for dry ice storage, and the Antarctic Treaty commanding international governance and scientific collaboration. Initial laboratory experiments of removing atmospheric CO_2 through deposition at surface pressure in a small prototype system resulted in

90% CO_2 depletion (Agee and Orton, 2016), which provides preliminary evidence of the simplicity in this approach.

While more advanced prototypes are necessary to evaluate the viability of this CO_2 removal process, the investigation of the response of meteorological phenomena to CO_2 sequestration in Antarctica takes precedence to assess CO_2 reduction effectiveness and associated consequences. Antarctic conditions can potentially be affected on shorter time scales than the 21st century time scale per the IPCC. The investigation will incorporate various sequestration scenarios with examination of CO_2 transport and meteorological response.

1.2 Background of CO_2 Transport and Anthropogenic Impacts

Observations show that atmospheric CO_2 concentrations have been increasing 1-3 ppmv annually from 1985-2015 (see Figure 1.1). Emissions have steadily increased (with the exception of the 2008-2009 year of the global economic recession) and are focused in areas of dense population and thriving economic activity. CarbonTracker (CT2019) is a model developed by NOAA that monitors sources and sinks of carbon dioxide through simulated atmospheric transport around the world to estimate surface fluxes of CO_2 with emphasis on North America. CT2019 estimates that 82% of fossil fuel emissions come from the northern extratropics, and about 87% of wildfire emissions come from tropical and southern hemisphere land. Natural sinks from the land and ocean take up about half of these emissions. From 2001-2018, CarbonTracker estimates the sum of natural fluxes composing of wildfire emissions, land sink, and ocean sink is only 49% of fossil fuel emissions. This means that the atmospheric growth rate would be doubled without the natural sinks.

This model developed by NOAA (as well as the NASA models i.e. "Following CO_2 through the Atmosphere") focuses on identifying locations of prominent sources and sinks to evaluate surface-atmosphere flux of CO_2 and resulting distributions. Aside from being important to study because of the greenhouse effect, CO_2 is an excellent tracer to evaluate atmospheric dynamics and transport. Once CO_2 has entered into the free troposphere, it sustains a long lifetime. For this reason, the literature holds information on how atmospheric general circulation transports carbon dioxide globally on various spatial and temporal scales.

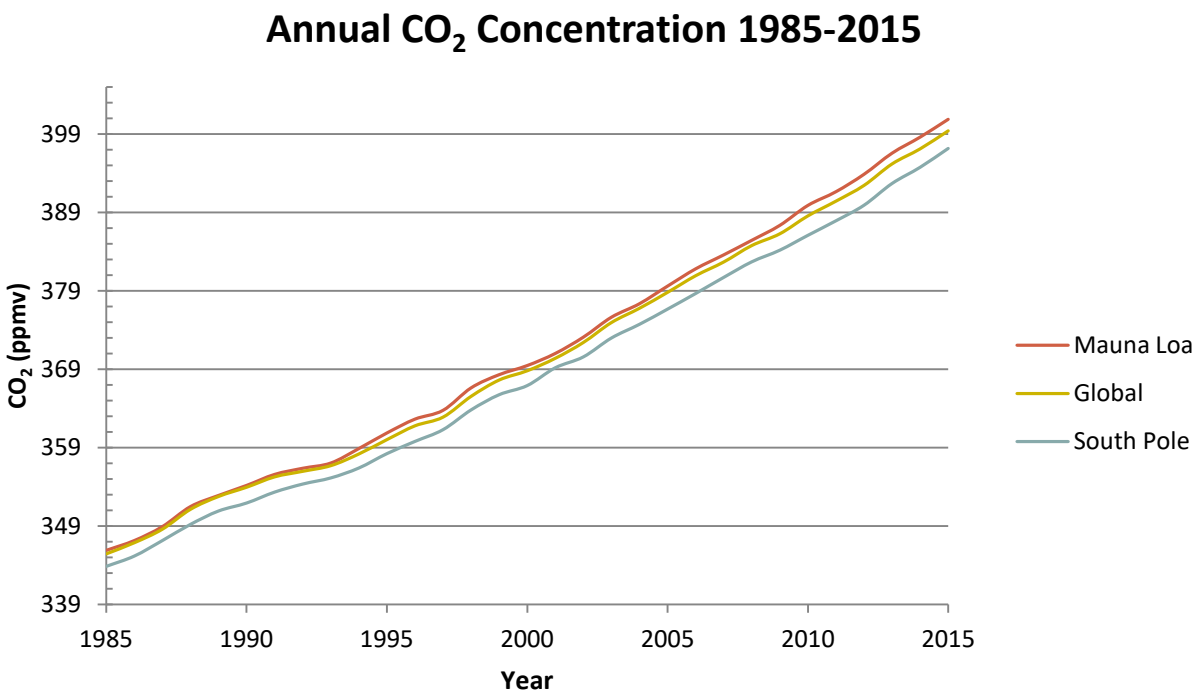

Figure 1.1. Annual increase of Mauna Loa, South Pole, and global CO_2 concentrations from 1985-2015 (NOAA ESRL Global Monitoring Division).

Miyazaki et al. (2008) conducted a comprehensive study of troposphere CO_2 transport incorporating all the sources and sinks. In general, the Southern Hemisphere has less concentration season variability in comparison to the Northern Hemisphere. Cross-equatorial eddies dominate the interhemispheric transport from north to south in boreal winter and spring, while the southward branch of the Hadley cell dominates the interhemispheric transport in boreal summer. The hemispheric transport is of interest to the study of CO_2 transport from the Northern Hemisphere to the Southern Hemisphere's engineered "CO_2 hole".

As shown in Figure 1.2, there is a concentration lag between the Mauna Loa and the South Pole Observatory. From 2000-2009, the CO_2 difference between Mauna Loa and the South Pole was on average 2.72ppmv which increased to 3.83ppmv for 2010-2015. Figure 1.2 also shows the lag in CO_2 concentration between Mauna Loa and the South Pole Observatory that has continued to increase throughout the 1959-2019 time period. The concentrations between the two measurement sites were comparable when measurements first started in 1959. One may question the ability of weather transport to keep up with the increasing anthropogenic

emissions to uniformly mix out the CO_2 concentration globally. Sequestration in Antarctica could increase this lag between the hemispheres.

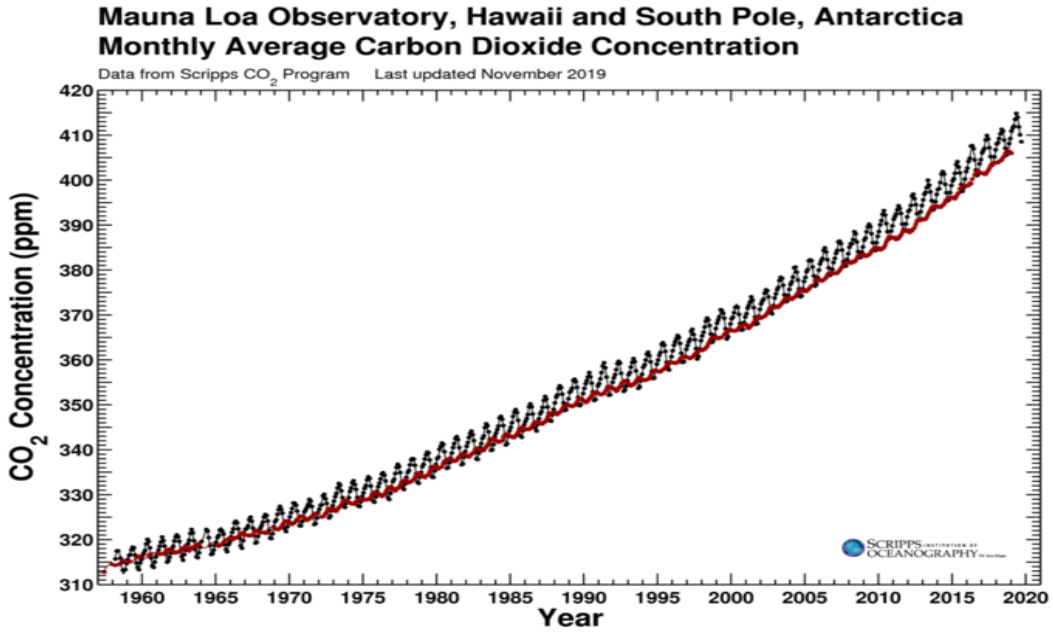

Figure 1.2. Scripps program CO_2 concentrations at Mauna Loa and South Pole observatory stations from 1958-2018.

As for troposphere-stratosphere exchange and stratospheric transport, Diallo et al. (2017) discusses how the Brewer-Dobson circulation is responsible for stratospheric poleward transport and troposphere-stratosphere exchange in the tropics. Since CO_2 acts as a coolant in the stratosphere, increasing concentrations cool the stratosphere and changes the Brewer-Dobson circulation. The Brewer-Dobson circulation aids in the transport of ozone to the poles (since ozone is primarily created in the tropics). Sequestering CO_2 could warm the stratosphere and affect this type of transport.

Ozone perturbations have been studied in models to evaluate radiative and dynamical response. Kiehl and Boville (1988) and Christiansen et al. (1997) examined sensitivity from imposed uniform ozone reductions and an ozone reduction scenario (not uniform) using January conditions. Results indicated that general circulation was most sensitive to uniform 100% reduction and the non-uniform "hole" reduction. These studies of ozone depletion and the resulting effect on the atmospheric circulation were motivated by the desire to understand the meteorological response to a change in radiative forcing. Numerous climate studies have been

conducted to consider the increase of CO_2 concentration as well as the decrease in CO_2 concentration.

Held et al. (2010) determined that an instantaneous return to preindustrial CO_2 forcing will not completely reverse climate change to pre-industrial climate. Cao and Caldeira (2010) examined the carbon cycle and climate response of instantaneous return (one time removal) to preindustrial concentration at year 2050 after following the IPCC A2 emission scenario. They found (using UVic ESCM 2.8) the control reached 1.8 ^{o}C above preindustrial by 2050 (at 511 ppmv of CO_2). After a few years of return to preindustrial concentration, the temperature decreased 0.8 ^{o}C. The additional 1^{o}C warming above preindustrial persisted for several centuries, meaning 100% removal of CO_2 offset less than 50% of the warming.

Boucher et al. (2012) examined hysteresis by transitioning from 1% increase in CO_2 concentration a year to 1% decrease in CO_2 concentration a year. Most metrics within the Earth system model study (HadGEM2-ES) showed hysteresis with respect to temperature and CO_2 concentrations such as low level clouds and ocean stratification in the Southern Ocean. MacDougall (2013) used the UVic ESCM to examine reversibility of Mirrored Concentration Pathways. After reaching peak concentration for the scenarios, the simulations do not return to 19th century temperatures by the end of the 30th century. Zickfield et al. (2016) shows that increasing emissions are more effective at warming than negative emissions are at cooling. Further, the study shows that negative emissions are less effective at cooling when applied to higher CO_2 concentrations.

In a recent study, Xu et al. (2020) examined the limitation of aridity over the Americas by using aerosol injections over limiting emissions and capturing carbon. It was determined that carbon capture is more effective in limiting the aridity of Americas but not as much as in the Amazon. This is important for the terrestrial hydroclimate response. Prescribed CO_2 concentrations were used in CAM5 for the CDR experiments and WACCM was used for the aerosol injection studies. Temperature change was comparable between the two strategies.

Tokarska and Zickfield (2015) examine emission scenarios that transition to net zero emissions and net negative emissions. UVic ESCM (2.9) was used and results show that it is possible to revert to a warming level of 2^{o}C above preindustrial with mitigation and CDR. However, thermosteric sea level rise is not reversible for at least several centuries and CDR efforts are opposed by outgassing from natural carbon sinks. Jones et al. (2016) studies the

carbon feedbacks of low emission scenarios with CDR. Results show that there is potential for reversal effect of the carbon cycle with these mitigation strategies, and more deployment of CDR will have to offset the outgassing from natural carbon cycles.

Depletion of atmospheric CO_2 from various CDR approaches have been examined in general circulation models and compared to one another for RCP scenarios per the IPCC. Keller et al. (2014) compared CDR approaches of afforestation, artificial ocean upwelling, ocean iron fertilization, ocean alkalinization, and solar radiation management during RCP scenario 8.5 with continuous climate intervention. The CDR approaches were found to be ineffective for limiting warming, but the solar radiation management scenario was found to have severe side effects of extreme rapid warming and an increase in atmospheric carbon dioxide when stopped. These results are consistent with the National Research Council 2015 documentation, however more CDR research needs to be conducted.

Keller et al. (2018) proposes the Carbon Dioxide Removal Model Intercomparison Project (CDRMIP) to address the need of enhancing the consensus on the atmospheric CO_2 reduction efficacy and climate impacts from different CDR technologies. The CDRMIP project will gather Earth system models in a common framework to explore impacts and challenges of CDR. The experiments under this framework (part of the CMIP6) are designed to examine reversibility, Earth system response to CDR, and potential impacts of reforestation, afforestation, and ocean alkanization.

1.3 Sensitivity Studies of CO_2 Sequestration in Antarctica

The understanding of CO_2 transport through atmospheric general circulation is very comprehensive as is the climate simulations predicting future climates based upon various emissions scenarios. Further, climate intervention studies inferring the mitigation effectiveness on current concentrations and future emission scenarios have been conducted for long term climate predictions. Cost of CDR is a huge obstacle for full installation of global CO_2 sequestration as is the potential limiting effects it has on reversing climate shown in model simulations. Assuming that cost and technology were manageable, there could be significant amounts of CO_2 sequestered in Antarctica through the AOR approach. Before reaching a global scale effort, it is imperative to study such climate intervention through using fully-coupled climate model simulations. Various scenarios will be considered using 21st century and future

SSP1-2.6 (Shared Socioeconomic Pathway, O'Neill et al. (2017)) conditions to evaluate the response of meteorological phenomena (which are responsible for CO_2 transport and seasonal weather) to atmospheric CO_2 sequestration in Antarctica.

CHAPTER 2. METHODOLOGY AND DATA

Examining the atmospheric response to CO_2 sequestration requires a highly sophisticated climate model to incorporate major Earth feedbacks. The land, ocean, carbon cycle, and atmosphere are all important parts to the various feedbacks. For this reason, the Community Earth System Model 2.1.1 has been employed for this study. Two categories of studies were conducted. The first category consists of different experiments containing modern day conditions with a) observed fossil fuel emissions with sequestration, b) no industrialization, and c) the control experiment with only observed fossil fuel emissions. The second category consisted of two separate experiments that continued the modern day experiments until the mid 21st century with SSP1-2.6 conditions (see below). One experiment continued the lesser sequestered scenario from the modern conditions and the other experiment continued the industrialization scenario. The same model version and components were used in both categories of experiments with the only difference being an update to the data for the future experiments.

2.1 Community Earth System Model 2.1.1

This version of the model is the latest release (Danabasoglu et al., 2020) as well as the model that performed all proposed experiments through NCAR's Coupled Model Intercomparison Project phase 6 (CMIP6). The model component parts are the same for both sets of experiments and includes the atmosphere (CAM6), ocean with biogeochemistry (POP2-ECO-ABIO-DIC), land with biogeochemistry (CLM5 BGC-CROP), land ice without evolution (CISM2), sea ice (CICE), river runoff (MOSART), wave evolution (WW3), and coupler. The wave and river runoff parts of the model were not modified in any of the experiments and were not considered during the analysis. There are two important features in this configuration for examination of CDR in Antarctica. One of the key tools in this configuration (B1850_BPRP is the compset name) is that the carbon cycle is prognostic for the ocean and land. In addition to the carbon cycle being utilized, the radiation linked to the CO_2 is also prognostic. For all component parts, twentieth century spin-up conditions were used to start the model (b.e20.BHIST.f09_g17.20thC.297_01) with additional spin-up time to allow for model

stabilization to initial conditions(see next section). Each model component requires different amounts of spin-up time. The BGC (land and ocean) takes several centuries to spin up but the atmosphere requires the least amount of spin up time. The components' stability relies on all other parts being stable. Therefore, data from previous NCAR experiments were used to initialize these experiments.

2.1.1 Community Atmospheric Model 6.0 (CAM)

This atmospheric component of this CESM configuration is a finite volume prognostic model with 32 levels. The grid used for all simulations was a 1 degree resolution (0.9 x 1.25). All input data for the namelist were selected based on the time period being considered. The short term simulations were conducted for the time period 2000-2014, and the Shared Socioeconomic Pathaway 1-2.6 time period was conducted from 2015-2049 (continued from selected 2000-2014 simulations). Other data within this component consisted of ozone, aerosols, and greenhouse gas concentrations. The radiation scheme was set to the default 'rrtmg.' The macrophysics, shallow convection, and eddy schemes were all set to the default 'CLUBB_SGS.' The most important feature in the CAM model for this research is that the radiation code is linked to the CO_2 tracer which responds to the changes in concentrations due to emissions, carbon cycle, and sequestration.

2.1.1.1 Short Term Simulation Set-up (2000-2014)

Twentieth century spin-up conditions were used for these simulations with an additional three years to stabilize with initial conditions. The data selected for all the variables in the prognostic part of the model were updated for the year 2000, and those data were recycled annually for all 15 years. These data include primarily ozone and aerosols. For the greenhouse gases shown in Table 2.1, all of them remained fixed except for CO_2 because its concentration was responding to industrialization, carbon cycle, and sequestration in Antarctica. The CO_2 concentration was initially set to the 1997 concentration, so that the emissions along with the spin-up would reach the 2000 concentration which equaled ~368 ppmv.

Table 2.1. Concentrations used in modern day simulations.

Greenhouse Gas	**Atmospheric Concentration**
CO_2	368.865 ppmv
CH_4	1751.022 ppbv
N_2O	315.85 ppbv
F11 (CFC)	676.052 pptv
F12 (CFC)	428.45 pptv

For the CO_2 emissions, the latest surface CMIP6 anthropogenic emission data were used for the CO_2 surface flux. The emission data are in units of kg m^{-2} s^{-1}. These data were also used to sequester out the CO_2 in Antarctica. The area of consideration was the latitudes 60^oS to 90^oS which encompassed the whole Antarctica region (surface area of 3.26×10^{13} m^2). Under the assumption that CO_2 sequestration could operate all hours of the day for every day of the year, the amount of CO_2 mass to remove from the entire atmosphere was calculated to reverse the concentration back to roughly Pre-Industrial (280-300 ppmv) in 15 years. This mass amount was then quantified over this surface area to remove CO_2 in the Antarctic region (negative emissions). The annual CO_2 removal for this "Full Sequestration" scenario resulted in ~9 ppmv (9.30 ppmv more precisely) reduction by sequestration in the atmospheric concentration. This is roughly $68.8BtCO_2$ removal a year. The second sequestration scenario for the short term simulations only sequestered half the amount of the "Full Sequestration" scenario, meaning ~4.5 ppmv (4.65 ppmv more precisely) or ~$34.4BtCO_2$ removal a year.

In the simulation where industrialization was shut off, the emission data were not used. This simulation can be thought of as a global society that has gone to complete renewable energy resources. The only changes to the CO_2 concentration were the natural sources and sinks of the land and ocean up taking the atmospheric CO_2.

2.1.1.2 Future Scenario with SSP1-2.6

The Shared Socioeconomic Pathways are predicted future scenarios that use Integrated Assessment Modeling (IAMs) to connect features of society and economic growth with the atmosphere and human activity (O'Neill et al., 2017). There are six categories incorporated into creating the SSP narratives that include environment and natural resources, technology, demographics, human development, economy/lifestyles, and policies/institutions. Determinant challenges to climate mitigation include energy and land use, advancement in technology, and policy enforcement. (O'Neill et al., 2017). These SSP narratives are the latest editions of the previous narratives known as the RCP and SRES (O'Neill et al., 2016). The SSPs will be included in the newest IPCC AR6 report due in 2021. There are five SSP narratives illustrated in Figure 2.1.

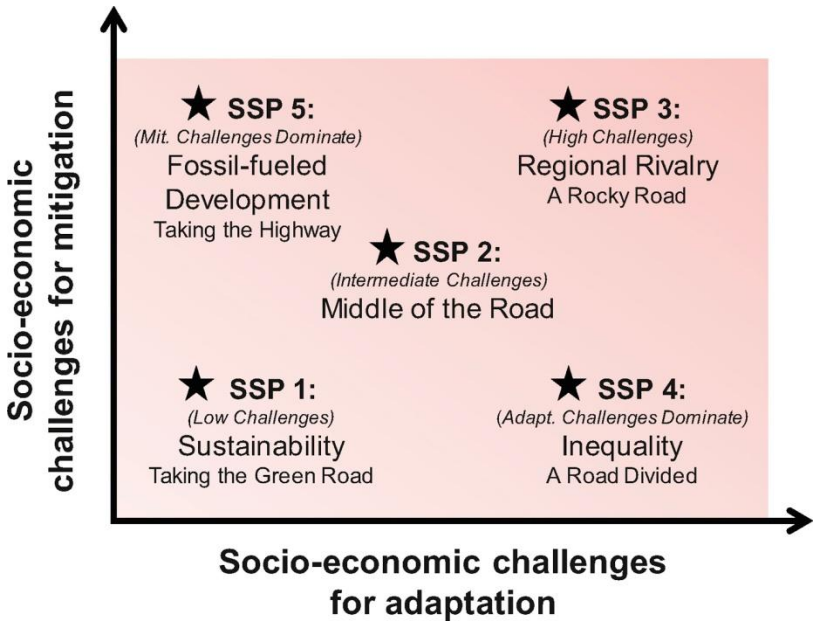

Figure 2.1. The various SSP narratives that consider different societal, economical, and political conditions going into the future. Figure taken from O'Neill et al.(2017).

The next set of experiments considers the SSP1-2.6 narrative which is similar to the RCP 2.6 scenario. The SSP1-2.6 is the sustainable narrative where society progressively leans toward respecting the environmental boundaries. This future society strives for renewable energy, green

technology, and international collaboration for low challenges for adaptations. Society becomes more resourceful, focuses less on economic growth, and manages a low population. Wealthier countries help under-developed countries to adapt an environmentally friendly strategy by providing financial resources, human resources, and new technologies. (O'Neill, et al, 2017).

There are two research experiments conducted in this category: the control with emissions continued from the 2000-2014 control run and the sequestration with emissions run continued from the 2000-2014 half sequestration run (~4.5ppmv removal a year). These simulations were continued until 2049 for 50 years total. All the namelist variables were updated with the SSP1-2.6 conditions. The CMIP6 SSP1-2.6 emissions were used for the simulations and sequestration was handled the same way as in the short term simulations. All other greenhouse gases were updated every 5-10 years based on the data from the RCP 2.6 (from GLADE database by Eaton and LaMarque, 2010). Each gas was averaged over a time frame to replicate the change over those 35 years. Figure 2.2 below shows these plots.

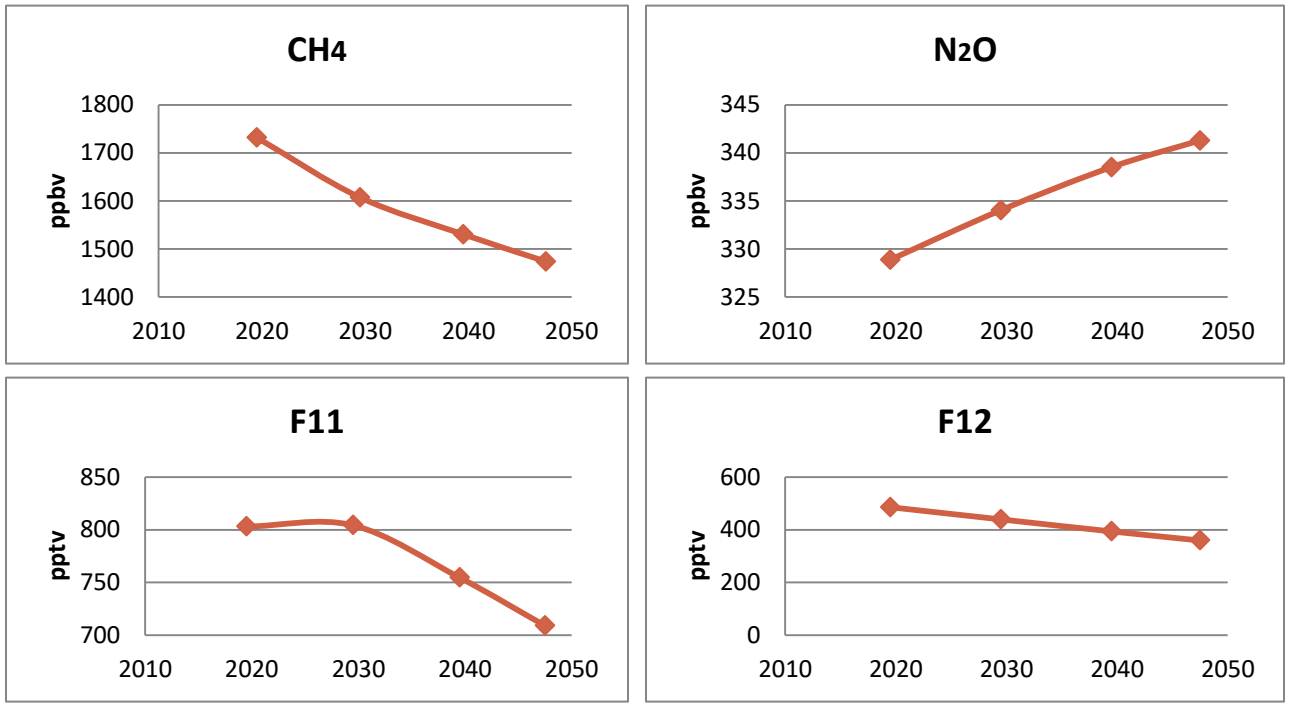

Figure 2.2. Time-centered values of greenhouse gases for the SSP1-2.6 simulations for 10 year averages (except for the last 5 years).

2.1.2 Parallel Ocean Program 2 (POP2)

The POP2 is the ocean model part of CESM, and was completely prognostic in temperature, dynamics, and CO_2 flux. This level-coordinate ocean general circulation model solves the three-dimensional primitive equations that describe ocean dynamics for a thin stratified fluid using hydrostatic and Boussinesq approximations. The grid for this model was the same for all simulations, and the 'gx1v7' mask was used. This grid is a displaced Greenland pole 1-deg resolution which removes the polar singularity problem. For the biogeochemistry part of the model, which provided the prognostic CO_2 from the ocean, the default configuration is MARBL that invokes the Biogeochemical Elemental Cycling (BEC) model. Ecosystem's component includes multiple phytoplankton groups, growth limiting nutrients, zooplankton, dissolved organic material, explicit simulation of the biogeochemical cycling of important elements, and sinking particulates. The ecosystem is coupled with a carbonate chemistry module that allows for dynamic computation of surface ocean pCO2 and air- sea CO_2 flux. (Smith et al., POP2 Reference Manual).

The 2000-2014 simulations were initialized with the year 2000 ocean conditions. When the "Half Sequestration" and control experiment were continued with as a SSP1-2.6 scenario, the ocean conditions were updated with SSP1-2.6 conditions. These conditions include the chemical variables within the ocean that contribute to the ecosystem of the ocean. All the modules for the ocean and BGC were left on default.

2.1.3 Community Land Model 5.0 (CLM5)

The land model component's role in the earth system model is to exchange momentum, energy, water vapor, CO_2, dust, and other trace gases between the land surface and atmosphere. This part of the model represents different characteristics of land surfaces such as soil texture, albedo, emissivity, vegetation type, surface roughness, leaf area index, cover extent, and seasonality. Along with representation of different types of land surfaces, it also depicts the changes and states of land surfaces such as soil moisture and temperature, canopy temperature, snow water equivalent, and carbon and nitrogen stocks. The BGC prognostic crop within the land model simulated the land portion of the carbon cycle in these experiments. The same grid resolution was used for all simulations (0.9 x 1.25), and the year 2000 conditions were set for the

land model in the 2000-2014 simulations. Conditions were updated for SSP1-2.6 conditions when the control and "Half Sequestration" simulations were forwarded into the SSP1-2.6 scenario. All modules were left on their default settings. (Andre et al., User's Guide of the Community Land Model).

2.1.4 Community Ice CodE (CICE 5)

The sea ice model is a dynamic-thermodynamic model that incorporates a subgrid-scale ice thickness distribution. Energy conserving thermodynamics are used and it has multiple layers in each thickness category. It accounts for the brine pockets influences within the ice cover. The default number of ice layers is 8 and for snow layers it is three. The freezing point at the sea ice-ocean interface is salinity dependent. The same grid resolution was used for all experiments, and the mask used was the same as the ocean.

2.2 Summary of Methods

These initial experiments for examining carbon dioxide sequestration in Antarctica are focused on the atmospheric response. The atmosphere, ocean, land, and sea ice are the active components in this configuration. The model configuration chosen represents major feedbacks that affect circulation and the data chosen represent the time periods of interest in this study. Evaluation of methods will be discussed in Chapter 5.

CHAPTER 3. RESULTS FROM 2000-2014 EXPERIMENTS

The first set of experiments for this CDR investigation is presented in this chapter. These set of experiments focus on modern day (2000-2014) that incorporate sequestration with observed anthropogenic emissions. The objective of the modern day simulations is to examine the sensitivity of atmospheric response to a variety of emission/sequestration scenarios. Global annual average CO_2 concentrations were globally weighted and pressure weighted. The 2-mair temperatures and downwelling longwave radiation were also globally weighted for the annual average. Analyses showing the global response with the map projection were completed using the AMWG diagnostics package from NCAR. Those computations were the difference between the last 5-years of simulation of the control (emissions only) and the other simulations of sequestration and no industrialization.

3.1 CO_2 Dispersion and Latitude Distribution

The global annual average CO_2 concentration for the four different simulations is shown in Figure 3.1. For continuity, the 1999 concentration (the same for all simulations) was incorporated with the time series data. The sequestration and no emission sensitivities were applied starting in January 2000. "Half Seq." refers to the ~4.5ppmv annual removal and the "Full Seq." refers to the ~9 ppmv annual removal.

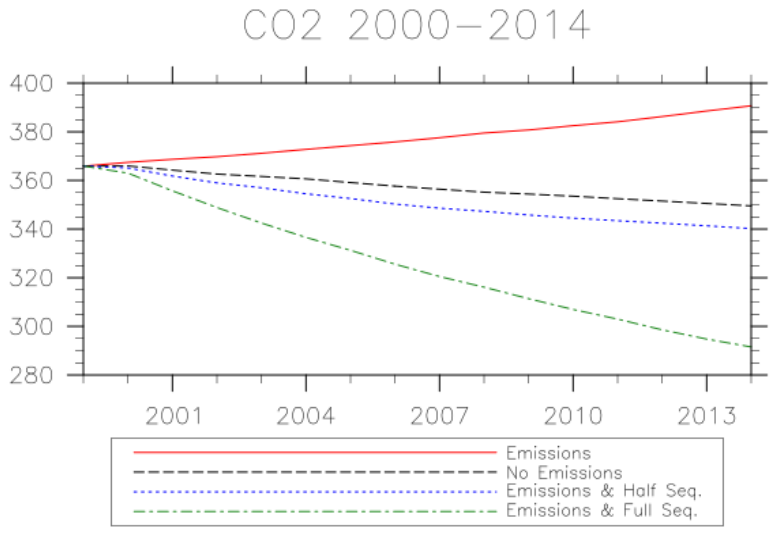

Figure 3.1. Global annual average CO_2 concentrations for various experiments from 2000-2014. The 1999 data point from last year of spin-up was used for continuity.

The "Emissions" simulation, defined as the *control*, shows a final concentration of ~390 ppmv, which is a 2-3 year lag from the 2014 observed global concentration of 397 ppmv. The concentration trend produced by the model is a good representation of the observed trend (see Figure 1.1). "No Emissions" simulation has the second highest final concentration of ~350 ppmv with "Half Seq." having a final concentration of ~340 ppmv. The full sequestration scenario has a final concentration of ~290 ppmv which is comparable to pre-industrial values. These results are all viewed as satisfactory evidence of CO_2 evolution given these emissions/sequestration scenarios.

The differences in hemispheric polar concentrations were quantified for all experiments. The purpose of this is to show how the heavy emitting northern hemisphere concentration compares to the sequestering southern hemisphere concentration. Figure 3.2 shows the control's polar difference (latitude bands 60^o-90^o in both hemispheres). The Mauna Loa and South Pole Observatory concentrations shown in Figure 1.2 have a comparable result for the same time period of the control experiment. Concentration difference between the polar regions resulted in ~4 ppmv, also viewed as consistent with observations.

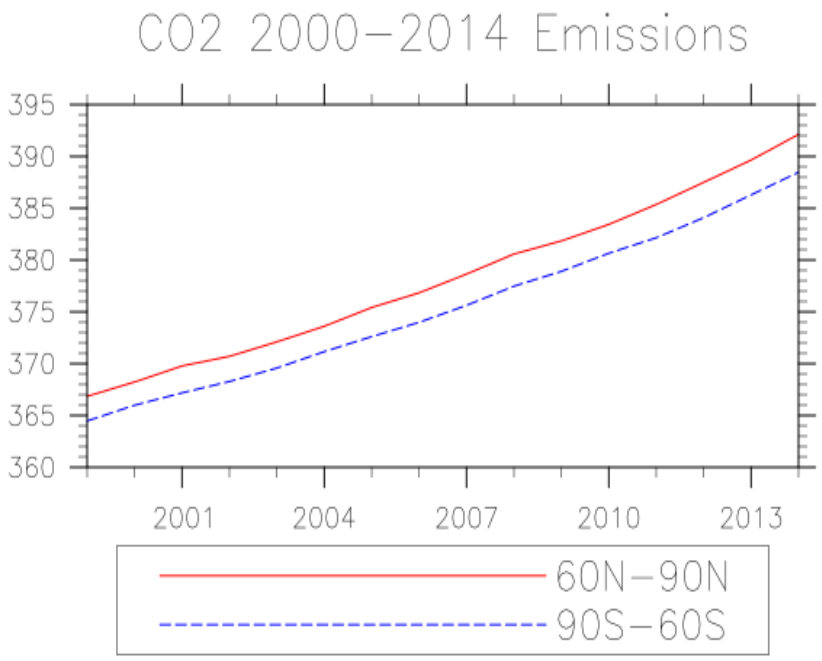

Figure 3.2. Concentration difference between the polar regions for the control simulation. Results are comparable to the Mauna Loa and South Pole observatory curves.

Figure 3.3 shows the polar hemispheric difference for the experiment without industrialization. After the first simulation year, the southern hemisphere polar concentration is higher than the northern polar concentration. While the lag between the hemispheres is smaller than the control's, there is a 1 ppmv difference between them. Having no emissions gives the carbon cycle the opportunity to reduce the atmospheric concentration. The concentration difference is potentially a result of the emitted CO_2 pre-2000 being in transit to the southern hemisphere before the industrialization shutting down. The continuous build up of CO_2 in the northern hemisphere was halted, and the atmospheric transport was able to balance out the concentration within a couple of years. This result is consistent with NOAA ESRL Carbon Tracker.

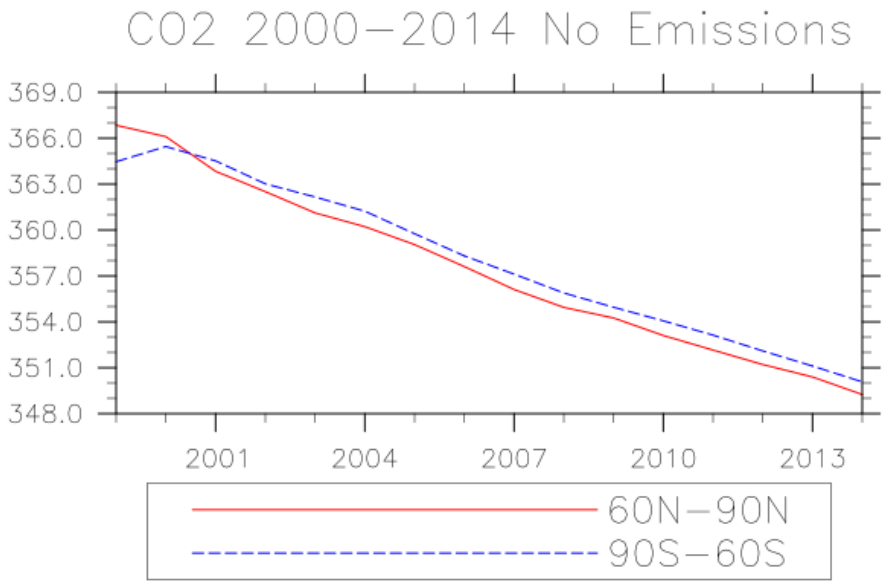

Figure 3.3. Concentration difference between the polar regions for the no emissions simulation. The southern hemisphere polar concentration is higher than the polar northern hemisphere.

The half sequestration experiment results are shown in Figure 3.4. Polar concentration difference resulted in ~10 ppmv. Sequestering in the southern hemisphere while also continuing industrialization enhances the existing CO_2 gradient between the hemispheres. The difference between them has more than doubled with that amount of sequestration. Considering the full sequestration experiment, Figure 3.5 shows that doubling the amount of sequestration doubles the half sequestration experiment difference between the hemispheres. The resulting difference in the full sequestration experiment is ~20 ppmv. Enhancing the CO_2 concentration difference

between the hemispheres also means a potential longwave downwelling radiation difference. Changing the CO_2 distribution from heavy sequestration at an isolated location can cause a change in the distribution of longwave radiation, potentially changing the weather pattern due to this forcing modification. Table 3.1 summarizes the hemispheric differences in the experiments.

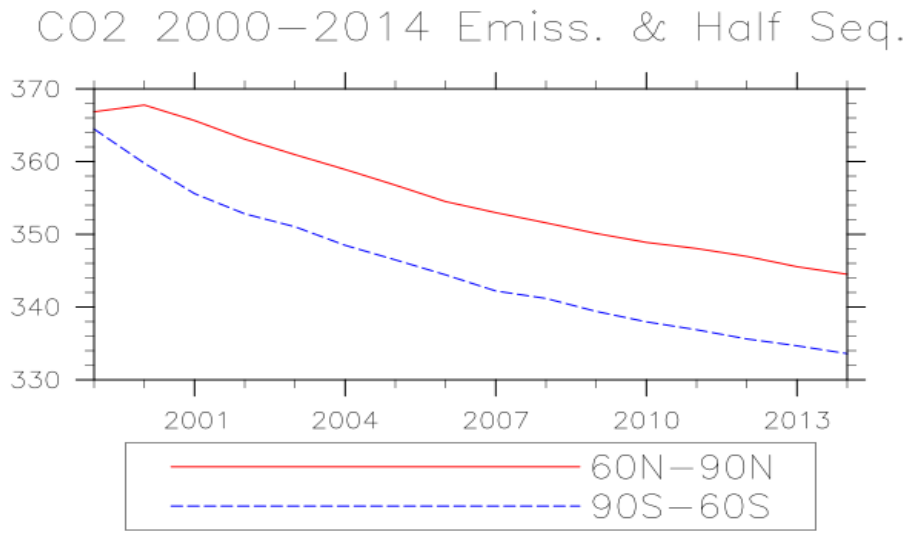

Figure 3.4. Concentration difference between polar regions for half sequestration simulation. The CO_2 gradient doubled with the Antarctica sequestration and ongoing emissions.

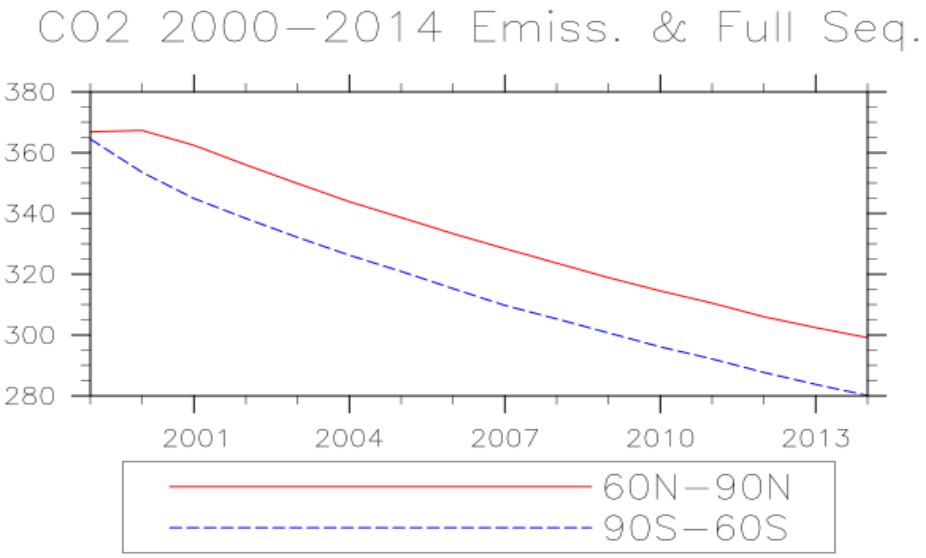

Figure 3.5. Concentration difference between the polar regions for the full sequestration simulation. This CO_2 gradient is over four times larger than the current observed one.

Table 3.1. Hemispheric polar differences at the end of each experiment. Sequestration enhances the existing gradient and shutting off industrialization shows the SH having a higher concentration ~ 1 ppmv.

Experiment	Polar Difference (NH-SH)
Emissions	**4 ppmv**
No Emissions	**-1 ppmv**
Emissions & Half Sequestration	**10 ppmv**
Emissions & Full Sequestration	**20 ppmv**

3.2 Meteorological Response

Temperature is the first signal one thinks of when considering climate change and mitigation strategies. Figure 3.6 shows the 2-m air temperature response throughout the 2000-2014 simulations (1999 data point included for continuity with spin-up). Results shows that the control had the highest temperature at the end of the simulation and the no emissions simulation had the second highest temperature. The sequestration experiments showed the lowest temperatures with the full sequestration having the lowest temperature of all the simulations.

The control simulation has a comparable result to the global average temperature of ~15^{o}C (288.15 K), which is ~1^{o} C above the pre-industrial average temperature (287.05 K or 13.9^{o}C). This is the 1 degree of warming due to anthropogenic emissions over the last century. Temperature results of the control show reliability of the model. At the end of the simulation, the difference between the final temperature of the control and full sequestration experiments is ~0.5 K. Between the half sequestration and control, the temperature difference is ~0.4 K with approximately the same result for the difference of the control and zero emissions.

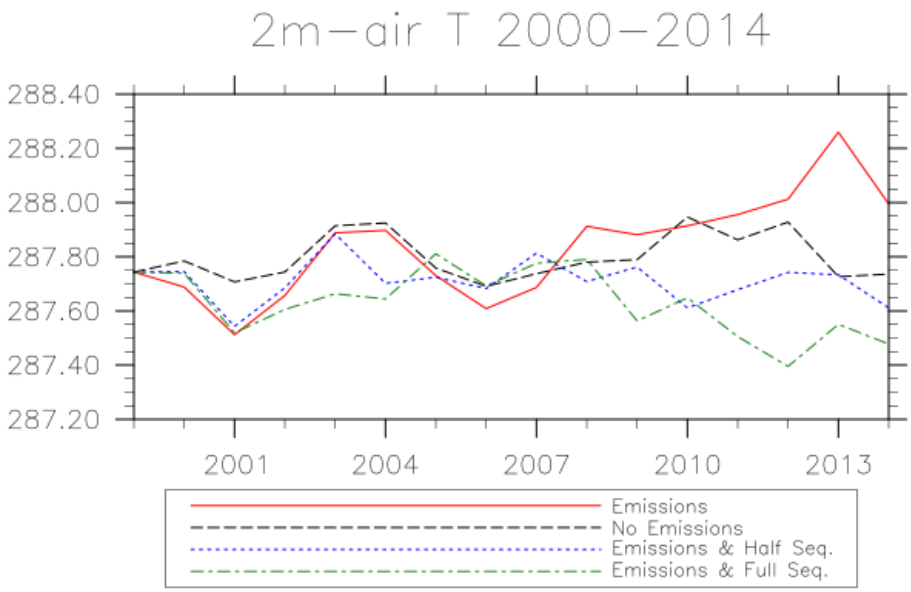

Figure 3.6. 2-m air temperature response to the various experiments for the 2000-2014 time period. The 1999 data point (spin-up) is included for continuity.

Though this is only a 15 year period, there is a signal for sequestering an ambitious amount of CO_2. In short term simulations, the chaotic behavior of the variables is expected due to both internal variability and the occurrence of any teleconnections. The no emissions experiment does show a lowering of temperature toward the end of the simulation but its temperature is comparable to the *control* until the last few years. However, all of the simulation temperatures during 2005-2008 are within 0.2 K of each other. The effect of reducing the CO_2 forcing appears to have the strongest signal toward the end of these simulations.

3.2.1 Downwelling Longwave Radiation

Removing and adding greenhouse gases to the atmosphere changes the amount of longwave radiation that escapes the atmosphere. When there is a higher concentration of greenhouse gases, longwave radiation absorbed will likely be reradiated back to the Earth's surface thus increasing the amount of downwelling longwave radiation at the surface. Sequestering CO_2 lowers the amount that is reradiated back to the surface. This cools the surface and less longwave radiation is emitted from the surface.

Figure 3.7 shows the global weighted average of the surface downward longwave radiation. The control has the highest amount and the full sequestration has the lowest amount. The sequestration scenarios have less CO_2 reradiating the longwave back to the surface but also

have cooler temperatures, so less longwave is being radiated. The change in downward longwave radiation and corresponding temperature change has been quantified for five latitude bands.

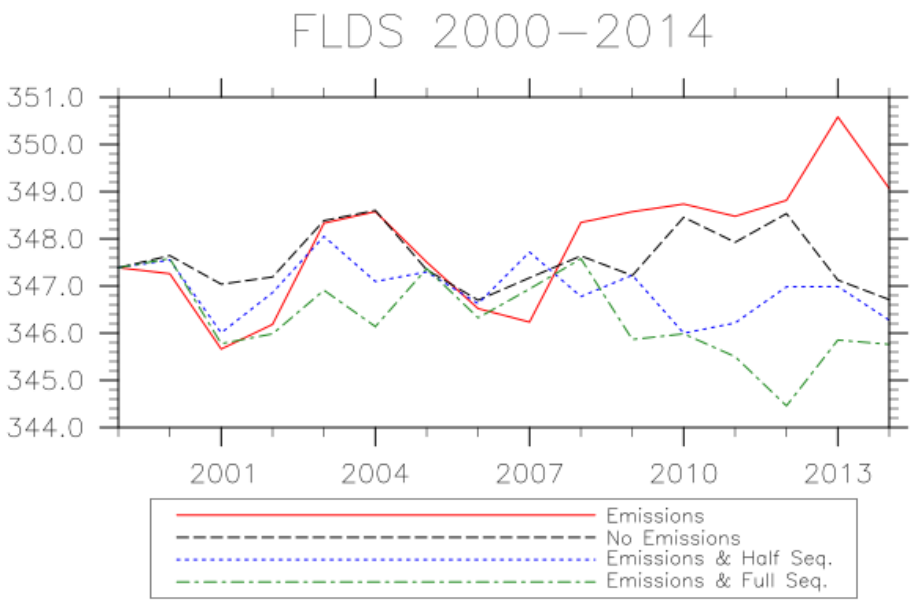

Figure 3.7. Global annual downward longwave radiation (W/m^2) for the 2000-2014 time period.

Figure 3.8 shows the downward longwave radiation and corresponding surface temperatures for the Antarctic region (60^oS-90^oS). The reduction in longwave radiation is ~4 W/m^2 by the end of the full sequestration experiment and temperature reduction is ~0.7 K. Antarctica is the coldest place on Earth thus having the least amount of longwave radiation coming from its surface. There is still a reduction in the amount of longwave reradiating back to the surface due to the sequestration. The Arctic region shows about the same resulting difference between the *control* and full sequestration as the Antarctic region.

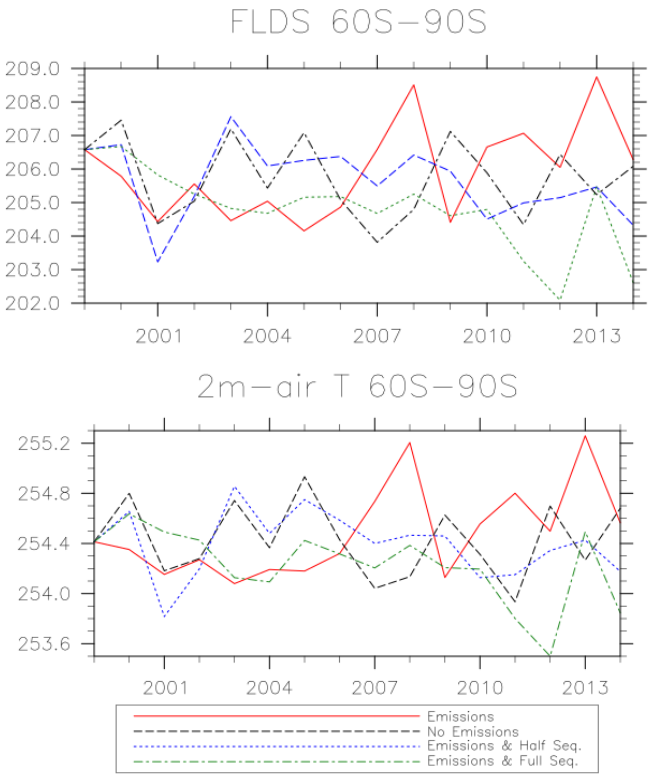

Figure 3.8. Downward longwave radiation and corresponding temperatures for 60°S-90°S.

In the northern hemisphere, the Arctic region has higher temperature and longwave radiation values due to it being warmer on average than Antarctica. Figure 3.9 shows the longwave radiation and temperature changes for the 60°N-90°N region. The temperature change between the *control* and the full sequestration is ~0.7 K and the longwave reduction to be ~4 W/m^2. The zero emissions and half sequestration experiments are comparable in temperature and longwave radiation throughout the simulation for both polar regions. Though there is an enhanced CO_2 gradient between the hemispheres with sequestration, the polar regions are responding the same amount in regards to temperature and longwave radiation.

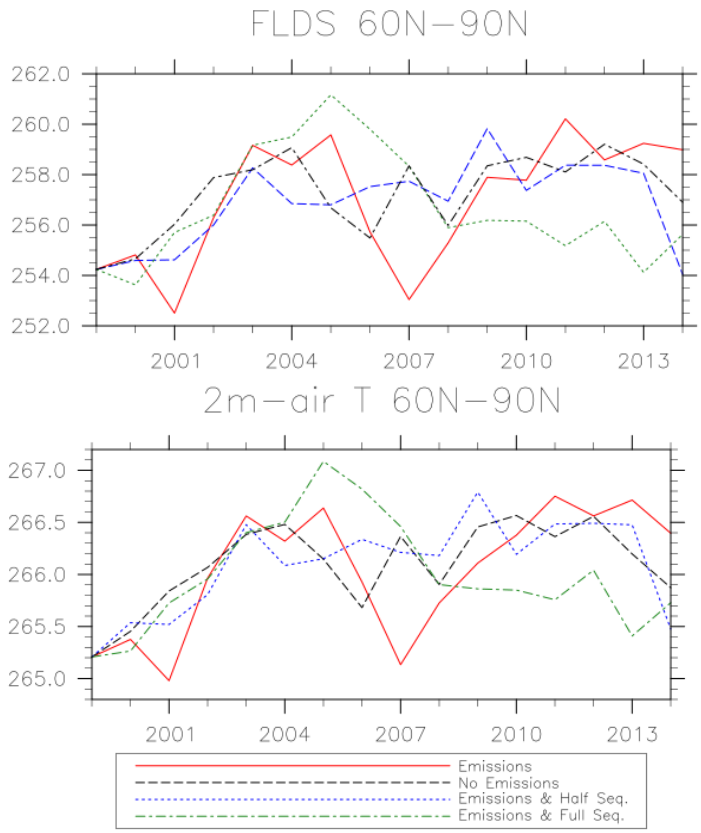

Figure 3.9. Downward longwave radiation and temperature for the 60°N-90°N region.

The midlatitude regions responded differently between the hemispheres. Northern hemisphere midlatitudes are majority land and in the southern hemisphere the midlatitudes are predominantly ocean. The ocean holds on to heat much longer than land surfaces. Surface property differences between those latitude regions account for the temperature and longwave radiation changes. Figure 3.10 shows that the southern hemisphere midlatitudes (30°S-60°S) has a similar response as the polar region with ~0.5K and 3 W/m^2 difference between the *control* and full sequestration. Figure 3.11 shows the northern hemisphere midlatitudes (30°N-60°N) that show a 1 K and 5 W/m^2 difference between the *control* and full sequestration experiments. Land heats and cools faster than ocean which explains the difference between the hemispheric response in those latitude bands.

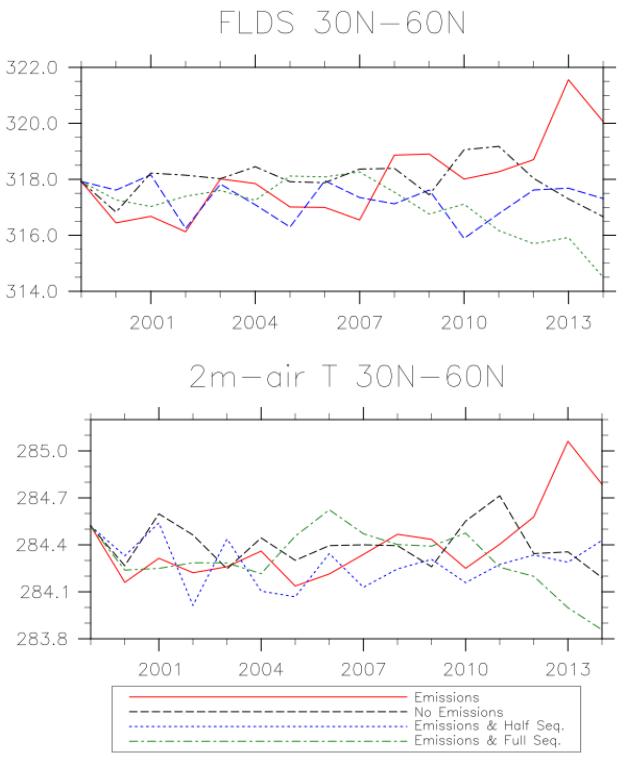

Figure 3.10. Downward longwave radiation and temperature for the 30°N-60°N region.

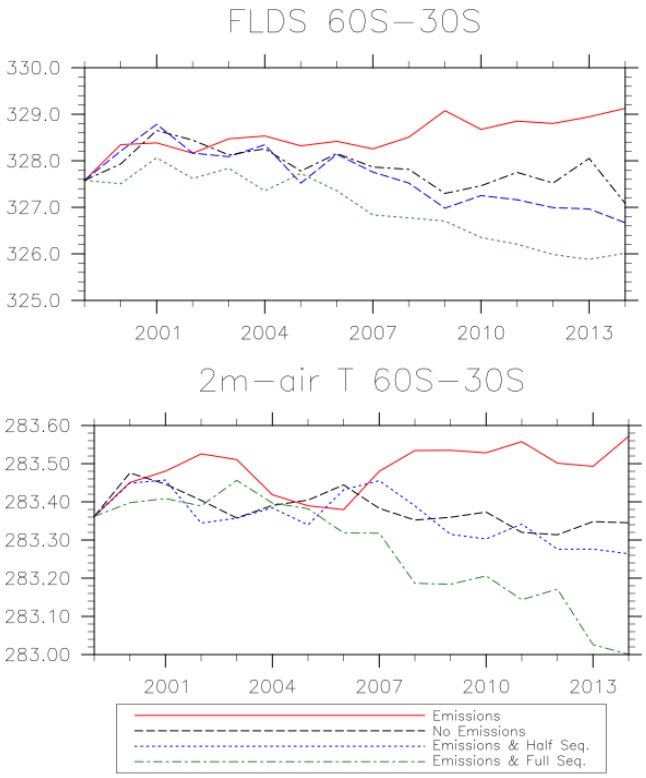

Figure 3.11. Downward longwave radiation and temperature for the 30°S-60°S region.

Lastly, the tropical (30°S-30°N) longwave radiation and temperature response are shown in Figure 3.12 below. The temperature difference between the final years of the *control* and full sequestration is ~0.3 K-0.5 K. The downward longwave radiation difference between those simulations is ~4 W/m^2. For the no emissions and *control* differences, the values for both are similar throughout the simulations. Sequestration had the strongest signal though it was in the range of 0.2 K-0.5 K.

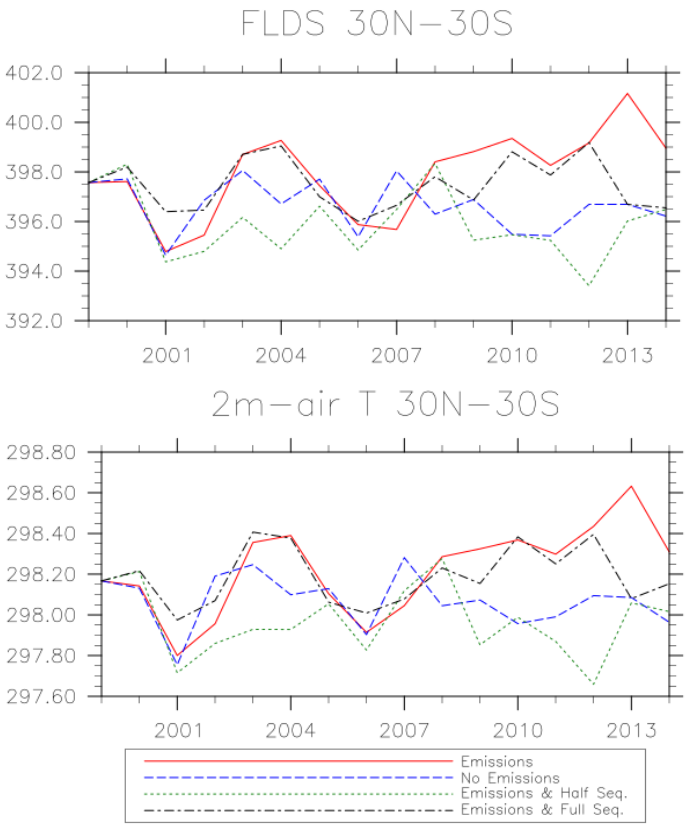

Figure 3.12. Downward longwave radiation and temperature for the 30°N-30°S region.

Northern hemispheric midlatitudes had the strongest signal with sequestration, though the rest of the latitude band regions were comparable in the amount of change between the *control* and full sequestration experiments. The simulation without emissions and *control* had comparable results with each other throughout the simulations. At times the half sequestration simulation did too. The full sequestration had the strongest signal in all latitude bands. In spite of the sequestration occurring the southern hemisphere, the forcing and temperature reduction was still occurring in the northern latitudes.

3.2.2 Global Response in Temperature and Precipitation

The average of the last five years was taken for the *control*, no emissions, half and full sequestration experiments. The change in meteorological variables from the *control* to each lowered CO_2 concentration simulation was found. Temperature and precipitation response are depicted for every location in the figures below. A fifteen year simulation is not a lot of data and an average of the last five years to determine the difference is even less. However, as shown in the temperature latitude response toward the end of the simulations discussed in Section 3.2.1, there is a global response to reduction of CO_2. Examination of other meteorological variables on this short term scale is therefore shown below for the no emissions, half and full sequestration experiments. These results are also suggestive of a need of simulation for a longer time period.

3.2.2.1 Global Temperature

Figure 3.13 shows the change in global annual 2-m air temperature from the control to turning off industrialization. There is a global decrease of 0.19 K by shutting off industrialization for 15 years. Strongest areas of cooling is in Eastern Asia, Africa, Australia, and Antarctica. Warming is shown in parts of the Arctic region and North America. These results could also be indicative of interannual variability associated with teleconnections that was not isolated in these experiments.

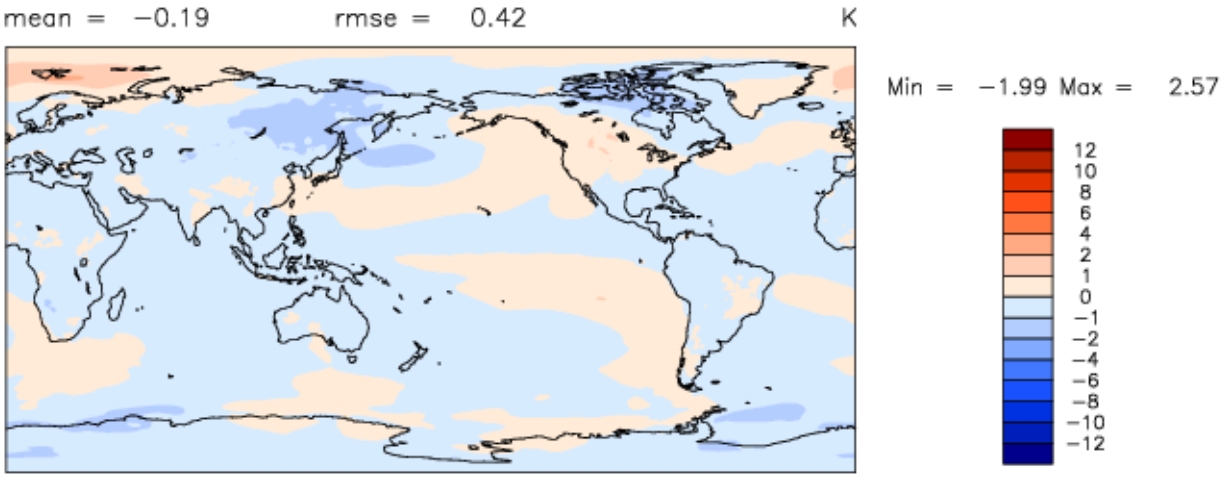

Figure 3.13. Five year averaged (2010-2014) difference: no emissions experiment minus *control* experiment. Annual global 2-m air temperature change.

Figure 3.14 shows the difference in the half sequestration experiment to the *control* for global annual average 2-m air temperatures. The CO_2 concentration difference between the no emissions and half sequestration end result is ~10 ppmv. Of all the simulations, the no emissions and half sequestration experiments are the closest in reduced CO_2 concentration. There is overall more cooling with a global average annual decrease of 0.35 K. There is much more cooling occurring in Antarctica than in the no emissions experiment. The half sequestration simulation result shows more wide spread cooling in Europe, North America, and Arctic region between North America and Asia. Southern hemisphere continents experience more cooling than the no emissions simulation as well.

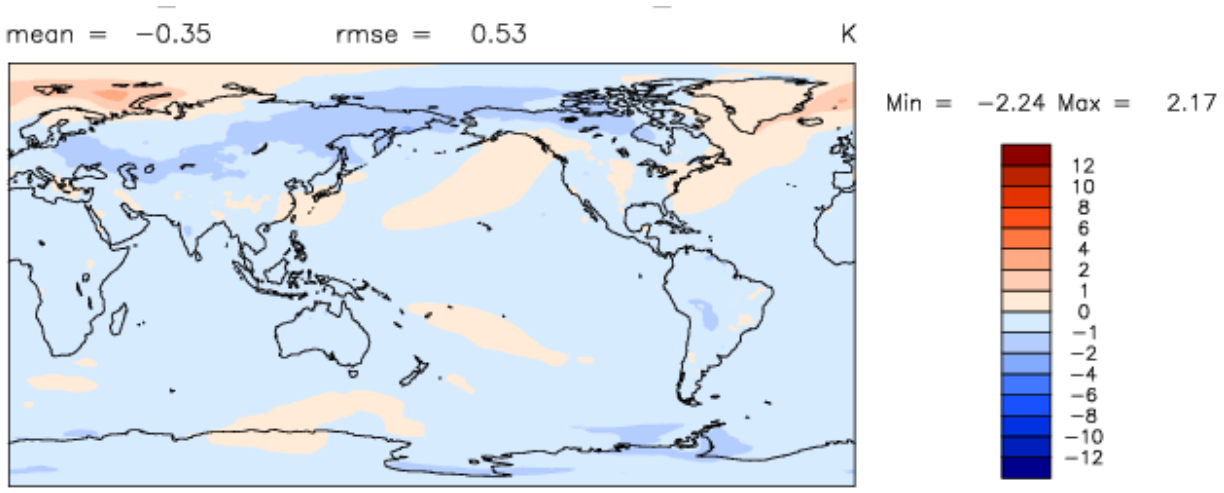

Figure 3.14. Five year averaged (2010-2014) difference: half sequestration experiment minus *control* experiment. Annual global 2-m air temperature change.

Figure 3.15 shows the change in temperature from the *control* to the full sequestration experiment. The global annual decrease in temperature in the final 5 years with full sequestration is 0.51 K. Similar areas of cooling are observed as in the change to shutting off industrialization and half sequestration. There is the most cooling over Antarctica of all the experiments, but the global concentration is comparable to pre-industrial. In the Arctic, there is uniform cooling in comparison to the other experiments and more cooling over the Midwest in North America. Australia, Africa, and South America experience amplified cooling seen in the half sequestration experiment.

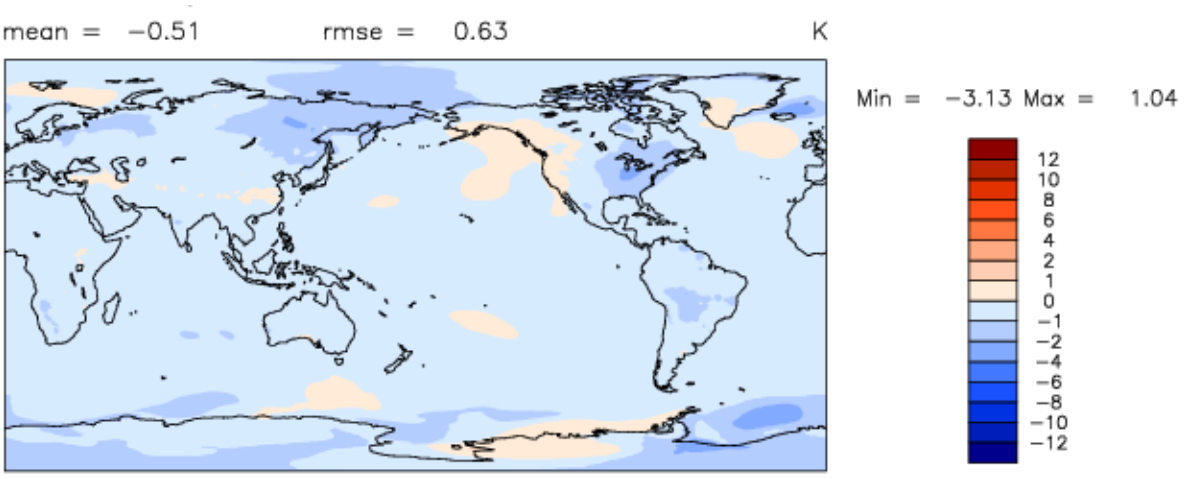

Figure 3.15. Five year averaged (2010-2014) difference: full sequestration experiment minus *control* experiment. Annual global 2-m air temperature change.

Uniform cooling is shown in the full sequestration experiment with enhanced cooling in the Arctic, North America, and Antarctica compared to the other experiments. The no emissions and half sequestration simulations are the closest in concentration to each other, but there is more cooling in the southern hemisphere. Shutting off industrialization had the least impactful effect on temperature in all the simulations because there was not as much CO_2 taken out. Precipitation has an overall weaker signal, and there was not a stronger signal with the full sequestration.

3.2.2.2 Precipitation

As with temperature, interannual variability can affect results, and five years of averaged data from a 15 year simulation may not cancel out the effects from teleconnections and associated interannual variability. However, there are precipitation differences noted between each type of reduction of CO_2 without there being a major reduction in annual precipitation accumulation. Figure 3.16 shows the global precipitation accumulation reduction of 0.23 cm in the no emissions scenario. There is decreased precipitation in North America and the majority of Africa, and increased precipitation is seen in the Pacific ocean, gulf, and South America.

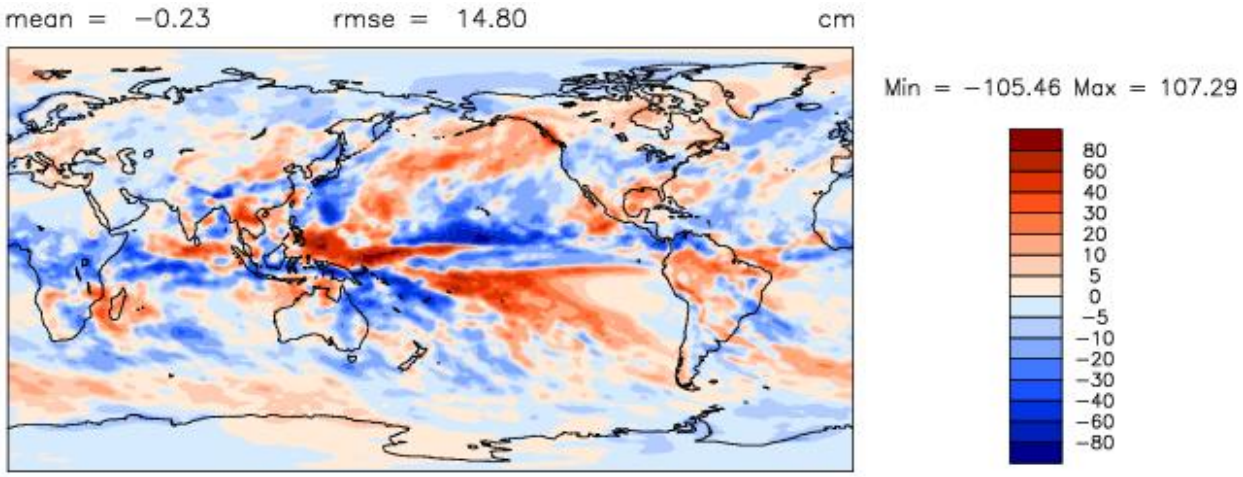

Figure 3.16. Five year averaged (2010-2014) difference: no emissions experiment minus *control* experiment. Annual global precipitation accumulation change.

Figure 3.17 shows the half sequestration effect on precipitation in comparison to the *control*. The global reduction is 0.53 cm in precipitation accumulation. There is a decrease in precipitation in the areas where there was an increase in precipitation in the southern Pacific ocean where the ITCZ and SPCZ are located. This could be simply a difference in teleconnections between the simulations. There are similar changes in precipitation patterns in the rest of world as in the no emissions scenario such as North America, South America, and Africa.

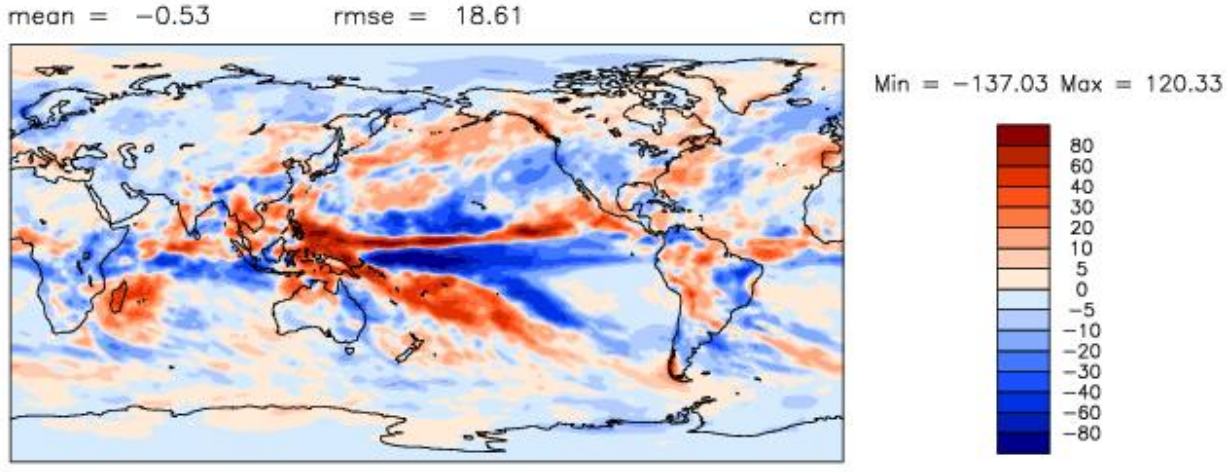

Figure 3.17. Five year averaged (2010-2014) difference: half sequestration experiment minus *control* experiment. Annual global precipitation accumulation change.

Figure 3.18 shows the full sequestration effect on precipitation accumulation. Interestingly, the global accumulation reduction is 0.32 cm. This is a smaller reduction than observed in the half sequestration experiment. There is a similar increase/decrease precipitation pattern in the southern Pacific as in Figure 3.17 but on a smaller magnitude. The strongest increase in precipitation is seen in Australia with full sequestration as opposed to the other CO_2 reduction scenarios. Similar patterns of increased precipitation in South America and the Gulf are observed as well as similar patterns of decreased precipitation in North America and Africa.

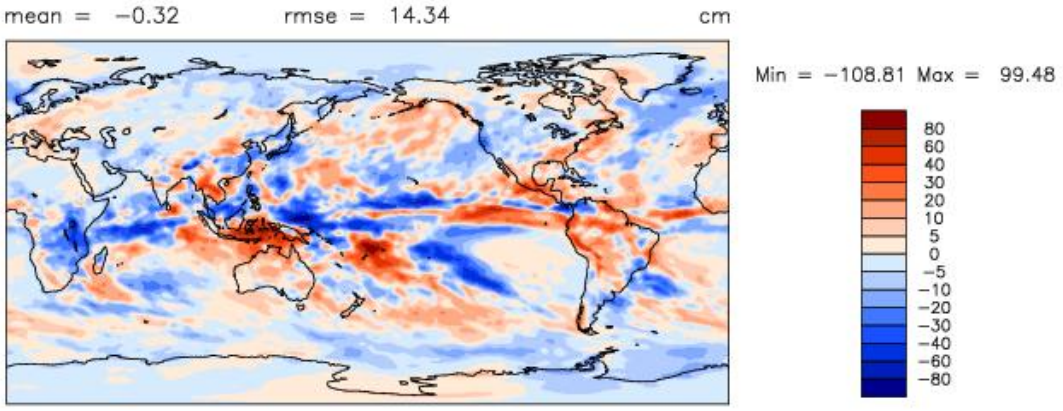

Figure 3.18. Five year averaged (2010-2014) difference: full sequestration experiment minus *control* experiment. Annual global precipitation accumulation change.

From all the scenarios, there is a consensus of less precipitation in Africa and North America, which is in agreement with Xu et al. (2020), and increased precipitation in South America, and the Gulf. The full and half sequestration simulations show a different change in precipitation pattern in the Pacific than the no emissions simulation. This could be simply due to teleconnections and interannual variability differences within each simulation. A longer run with ensembles would give more data to distinguish the signal more clearly. However, the continental changes are mostly in agreement between all simulations.

As discussed in the next chapter, the *control* and half sequestration simulations are continued into the mid 21st century with SSP1-2.6 conditions. These simulations each have 50 years of data to provide a more thorough dataset for analysis. For the short term simulations, temperature appears to have the strongest signal. Up to a 0.5 K in global temperature reduction was observed in the experiments as well as a modest decrease in global precipitation. The same variables in addition to others will be examined in the fifty year simulations.

CHAPTER 4. RESULTS FROM SSP1-2.6 EXPERIMENTS

The set of experiments presented in this chapter consider the modern day simulations continuing in the future (2000-2049). The modern day control (observed anthropogenic emissions) and half sequestration (observed anthropogenic emissions with 4.5 ppmv sequestered annually) are continued forward from 2015 along a socioeconomic path that considers society limiting emissions and being more environmentally conscious. The Shared Socioeconomic Pathway 1-2.6 scenario is the most sustainable future described of all SSPs. According to SSP1-2.6, the radiative forcing increase relative to pre-industrial peaks at 3 W/m^2 by mid-21st century and decreases to 2.6 W/m^2 by the end of the 21st century. The concentration for CO_2 reaches ~450 ppmv by 2050 and from there society takes action to limit emissions so that the concentration levels off. The *control* and half sequestration experiments from the 2000-2014 time period are continued forward with SSP1-2.6 emissions and conditions until 2049 for a total of fifty years. The half sequestration maintains the same amount of annual sequestration in Antarctica.

4.1 CO_2 Dispersion and Hemispheric Difference

Figure 4.1 shows Earth's pressure and global weighted annual average CO_2 concentrations. The results show the *control's* concentration reaching ~445 ppmv by the mid-21st century, and the sequestration's concentration nearing ~305 ppmv. In the SSP1-2.6 scenario, emissions accelerate between 2020-2040, and one can see the sequestration's effect on the concentration slows during those decades until emissions slow down toward 2050. By the end of the simulation, there is a CO_2 difference of ~140ppmv between experiments.

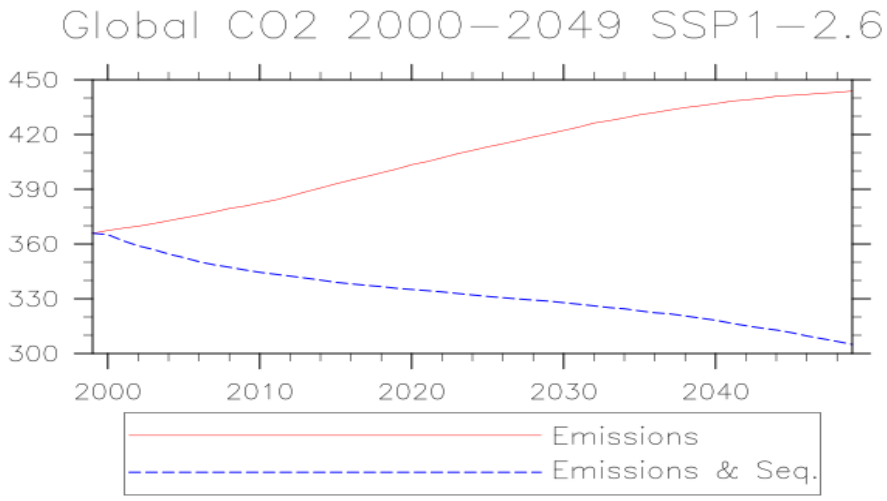

Figure 4.1. Global annual average CO_2 concentrations following the SSP1-2.6 (started in 2015). There is a CO_2 difference of ~140 ppmv between the *control* and sequestration.

The polar difference between the hemispheres was quantified for both simulations. Figure 4.2 shows the *control's* hemispheric concentration difference. The lag between the hemispheres increases for a decade after 2015 due to the increase in emissions, but the lag decreases by 2050 due to the limit in emissions imposed by society. By the 2040s, the lag between the hemispheres is the smallest of the entire time period.

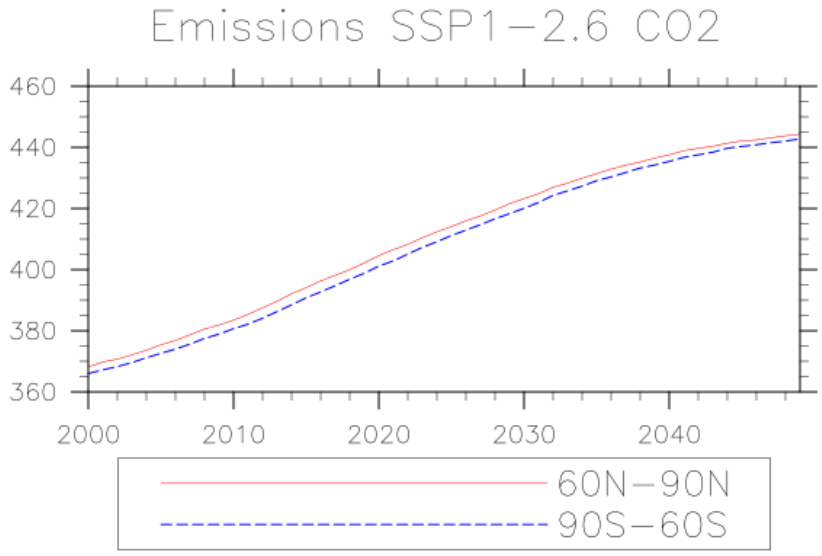

Figure 4.2. Polar hemispheric concentrations for the *control* simulation. The lag is the greatest from 2015-2030.

For the sequestration simulation, the polar hemispheric difference was maintained as seen in the 2000-2014 time period. Figure 4.3 shows the 2000-2049 polar concentrations for both hemispheres. As in the *control*, there is an increased lag during 2015-2030 due to the increasing emissions associated with this scenario. The lag is ~10 ppmv throughout the remainder of the simulation with the Antarctic region having 300ppmv and the Arctic having 310 ppmv.

Table 4.1 summarizes the hemispheric CO_2 gradients observed by 2049. Limiting emissions in toward the mid 21st century starts to decrease the lag between the hemispheres but a larger lag is continued with sequestration occurring in Antarctica. By having more data with this CO_2 gradient between the hemispheres, temperature and downward longwave flux can be examined to see if there's a long term effect of having this significant amount of sequestration annually in the southern hemisphere.

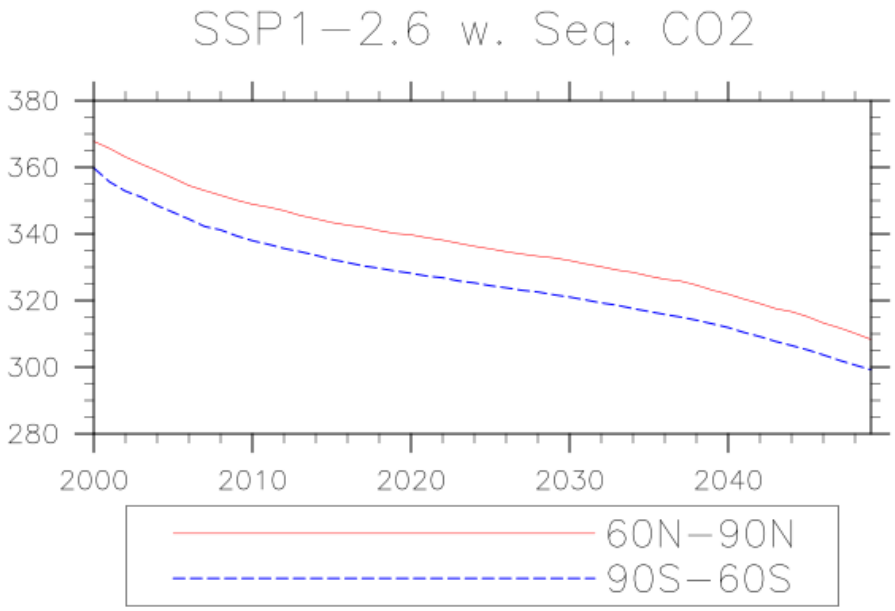

Figure 4.3. Polar hemispheric concentrations for the control simulation. The lag is the greatest from 2015-2030.

Table 4.1. Summary of hemispheric CO_2 gradients in 2049.

Experiment	Polar Difference (NH-SH)
Emissions	**2 ppmv**
Emissions & Sequestration	**10 ppmv**

4.2 Meteorological Response

There is a significant difference in CO_2 concentration by 2049 between the two simulations. Because of that difference, the meteorological response in each experiment will be different due to the different amounts of CO_2 forcing. Figure 4.4 shows the global annual average temperature for both experiments. The *control* shows a final temperature of 288.8 K which is ~0.75 K greater than the modern global average temperature. By sequestering CO_2 and abiding by SSP1-2.6, the 1°C of warming agreed upon in the Paris Agreement can be prevented.

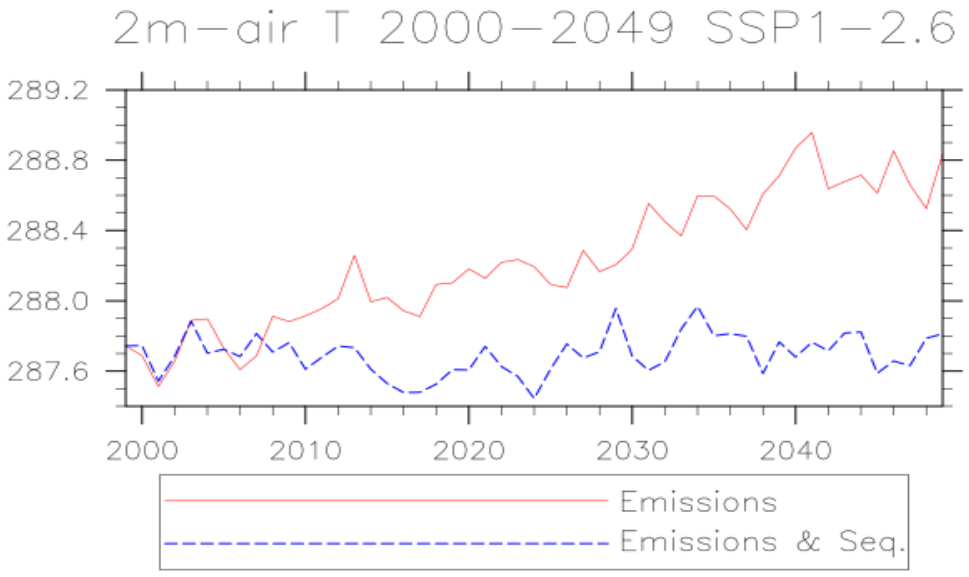

Figure 4.4. Annual global 2-m air temperature for the *control* and sequestration for SSP1-2.6. One degree of warming is prevented with sequestration.

4.2.1 Latitude Temperature and Downward Longwave Response

Latitude band changes in downward longwave flux and 2m-air temperature has been quantified for comparison. In the 2000-2014 time period, response to heavy sequestration was essentially uniform for all the latitudes. For a longer time period, more information is provided to examine the potential of uniform response to southern hemisphere sequestration. Figure 4.5 below shows the global annual average downward longwave radiation. By the end, there is a 7 W/m^2 difference between the simulations. The sequestration simulation stayed within the 346-348 W/m^2 range and the *control* increases at least 7 W/m^2. In the full sequestration scenario discussed in Section 3.2.1, the downward longwave radiation is the same amount as shown throughout the duration of the SSP1-2.6 sequestration. Sequestration prevented any increase of downward longwave radiation.

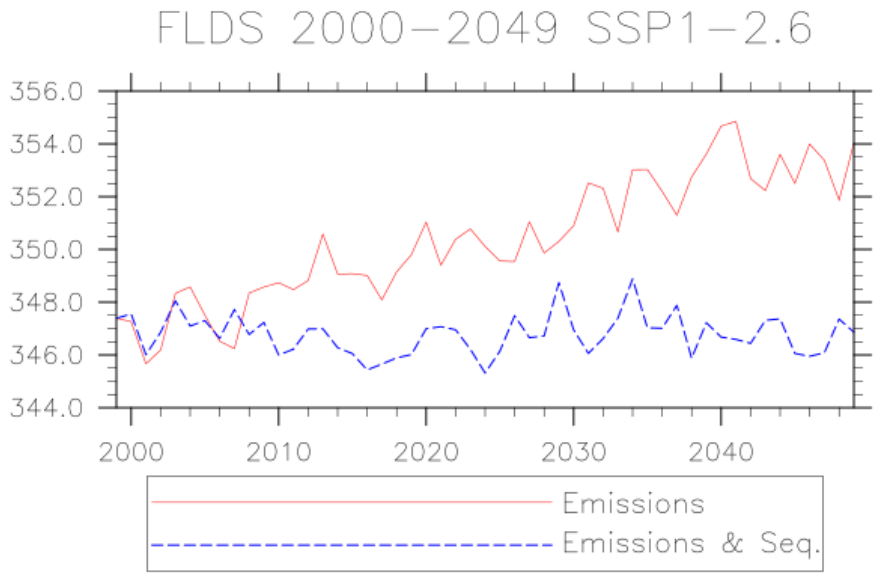

Figure 4.5. Global annual average downward longwave radiation for both SSP1-2.6 simulations.

The latitude bands discussed in Section 3.2.1 are also examined for this set of experiments. Figure 4.6 shows the northern hemisphere polar region temperature and downward radiation change.

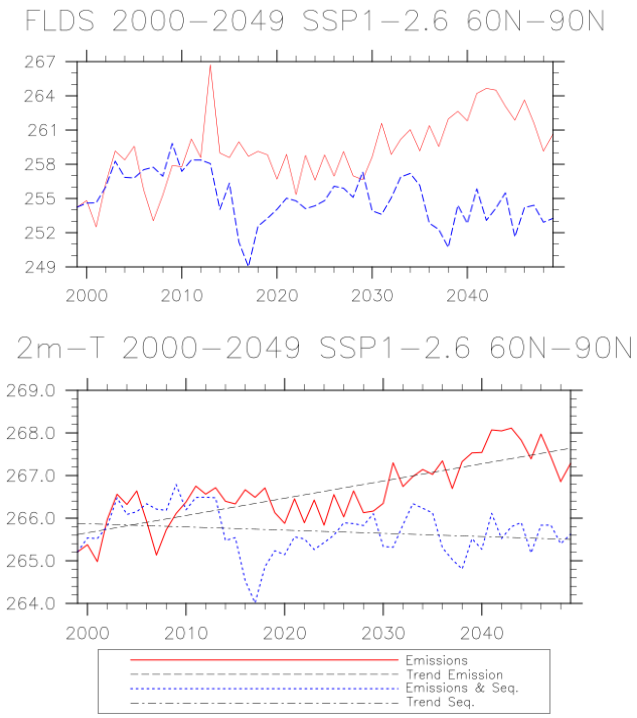

Figure 4.6. Annual average 60°-90°N downward longwave radiation and 2-m air temperature for SSP1-2.6.

By 2049, there is a 6-7 W/m^2 difference between the experiments and the 2-m air temperatures differ by 2-3 K. Figure 4.7 shows the northern hemisphere middle latitude downward longwave radiation and temperatures. The temperature difference between the experiments is 1-2 K and the downward longwave radiation is 6-7 W/m^2.

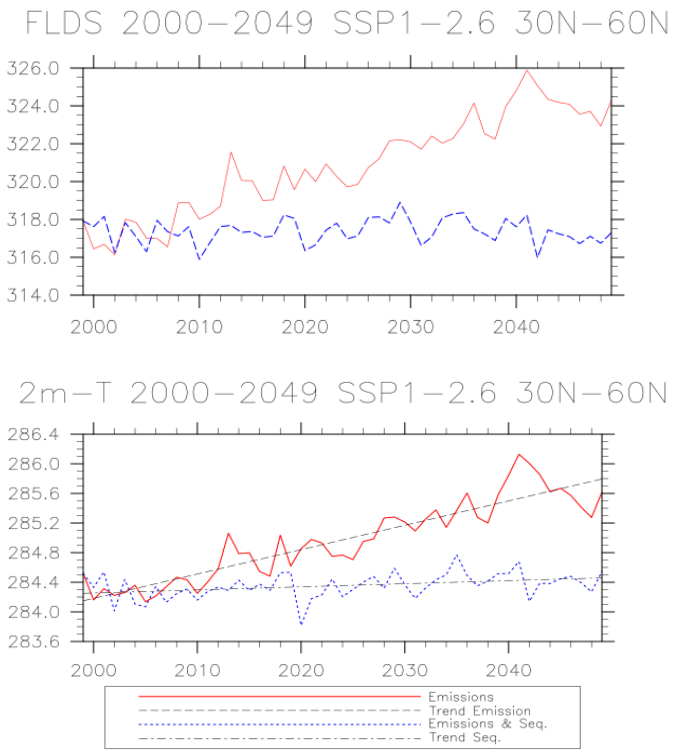

Figure 4.7. Annual average northern hemispheric middle latitude downward longwave radiation and 2-m air temperature.

Tropical latitude longwave radiation and temperature changes are shown in Figure 4.8. Temperature change is ~1K and downward longwave radiation is ~8 W/m^2. The predominantly ocean southern hemisphere middle latitude response in downward longwave radiation and 2-m air temperature is shown in Figure 4.9. Sequestration prevents 0.8 K of warming in those latitudes and 5 W/m^2 increase in downward longwave radiation. As for the southern hemisphere polar region shown in Figure 4.10, sequestration prevents 5-7 W/m^2 increase in downward long wave radiation and 1-1.5 K temperature increase.

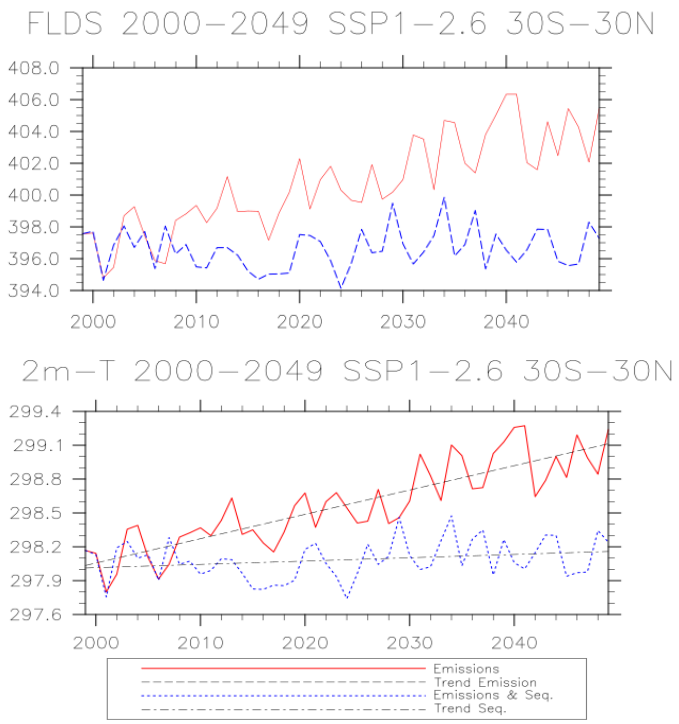

Figure 4.8. Annual average tropic downward longwave radiation and 2-m air temperature.

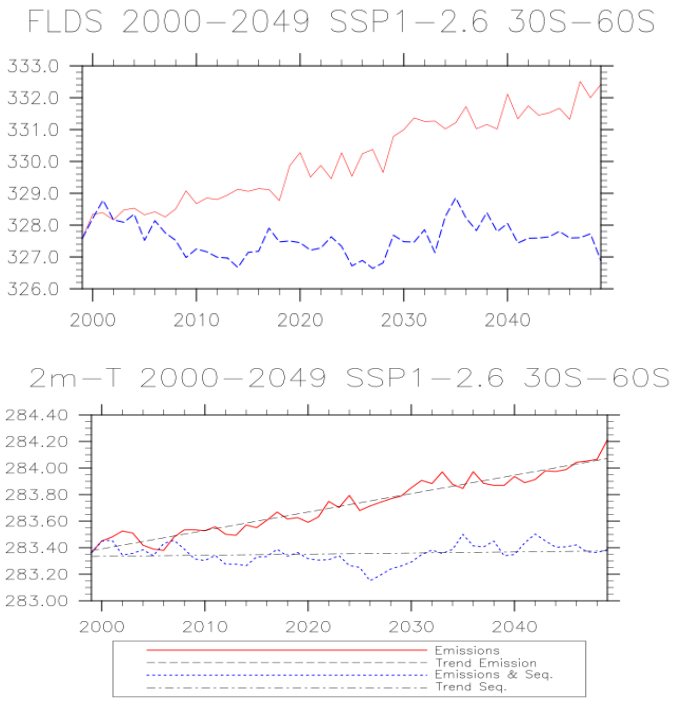

Figure 4.9. Annual averaged southern hemisphere downward longwave radiation and 2-m air temperature.

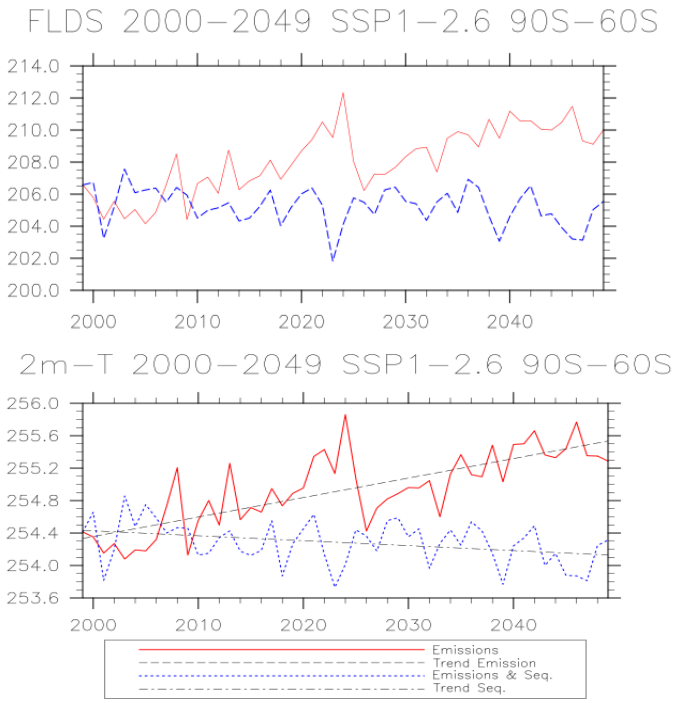

Figure 4.10. Annual average southern hemisphere polar region downward longwave radiation and 2-m air temperature.

Both polar regions have a downward trend in temperature of ~0.5 K due to sequestration throughout the 50 year period. The other latitude bands maintain or show a slight decrease in the temperature trend throughout sequestration. The *control* shows a 1-2 K increase in temperature for all latitude bands throughout the time period. Increasing the atmospheric CO_2 roughly 50 ppmv in 35 years strongly affects the temperature signal, and sequestering maintains or decreases the temperature. The polar regions have the strongest temperature response is explained by polar amplification, or rather deamplification, with sequestration. The polar regions are the most sensitive to warming compared to other parts of the world (IPCC, 2013). The change in temperature between the experiments will change other meteorological variables such as wind and precipitation. These signals are examined in the following section to show the sequestration's change to climate change.

4.2.2 Changes in Global Patterns of Temperature, Wind, and Precipitation

The final 10 years of both experiments were averaged, and the change between meteorological variables was quantified. Figure 4.11 shows the global temperature difference between the simulations. The strongest response to sequestration in preventing warming is located in the North America, the Arctic, northern Europe, and parts of Antarctica. These locations have a preventative temperature difference of 2-4 K. Sequestration prevents Australia, the Middle East, and Africa from warming 1-2 K and majority of the oceans are prevented from warming 1 K.

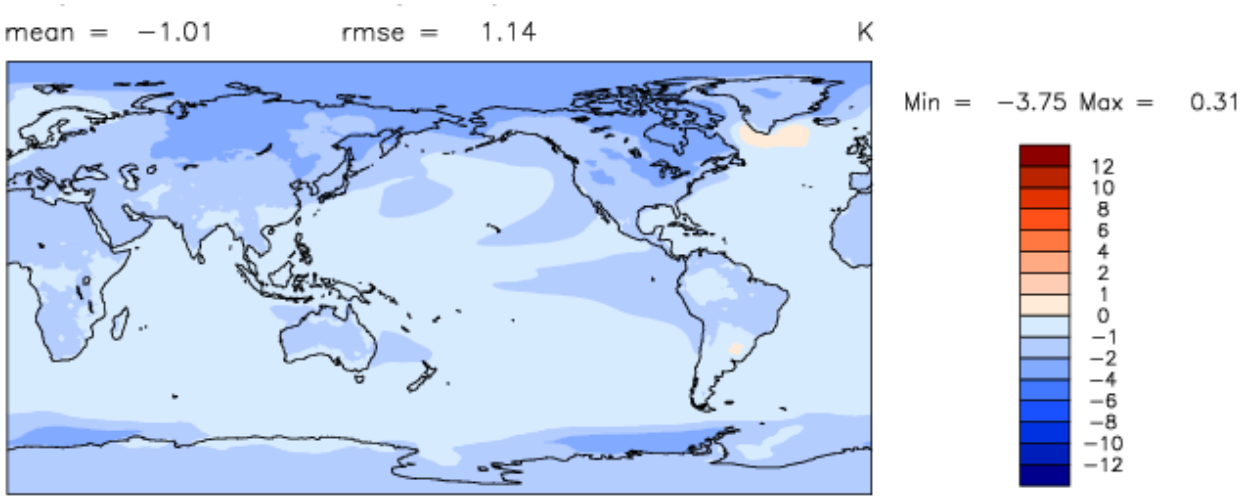

Figure 4.11. Averaged final 10 years difference in 2-m air temperature. Emissions with sequestration minus control.

The final 10 year average annual temperature for the sequestration experiment is 287.74 K and the *control's* is 288.74 K. The *control* is 0.70 ^{o}C higher than the current global average of 14.9 ^{o}C, which is comparable to the 1.5-2^{o}C increase to pre-industrial temperatures that the SSP1-2.6 predicts. Figure 4.12 shows the global mean monthly difference in temperature between the experiments. Every month shows a 1 K difference, but June, July, and August shows a 1-1.5 K change.

Figure 4.13 shows the vertical temperature change at all latitudes and the change in zonal wind. There is uniform cooling in the troposphere and warming in the stratosphere compared to the *control*. CO_2 acts as a coolant in the stable stratosphere layer, so lower CO_2 concentrations will not cool the stratosphere in a continuously emitting scenario. There is little change in the

zonal wind in the troposphere, which is consistent to the uniform preventative warming effect of sequestration. A strong temperature gradient change would perhaps affect the zonal wind more. There is also weakening of zonal wind in the stratosphere, mostly in the southern hemisphere, which corresponds to sequestration's preventative cooling on the stable layer.

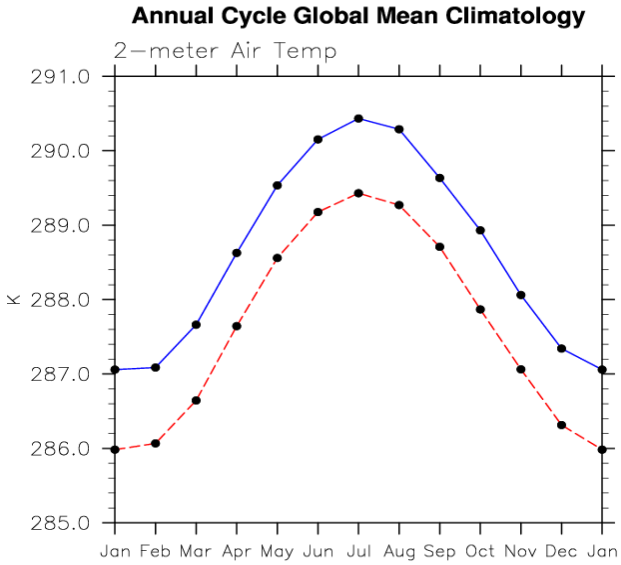

Figure 4.12. Global temperature average for each month. Sequestration prevents at least 1 ^{o}C of warming for each month.

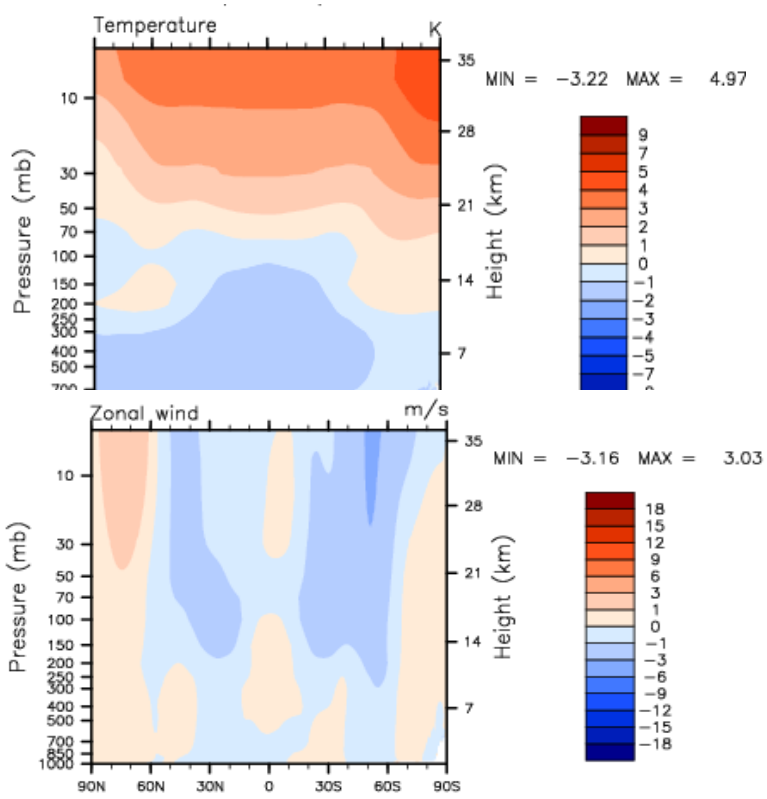

Figure 4.13. Annual average vertical temperature and zonal wind changes.

Global annual average precipitation accumulation differences is shown in Figure 4.14. Sequestration prevents globally 1.57 cm of accumulation a year which is ~0.6 in. Patterns show an increase in precipitation in northern parts of South America, northern Africa, western Australia, Atlantic Ocean, and the SPCZ by incorporating sequestration. There is drying observed in North America, parts of Australia, and in the ITCZ.

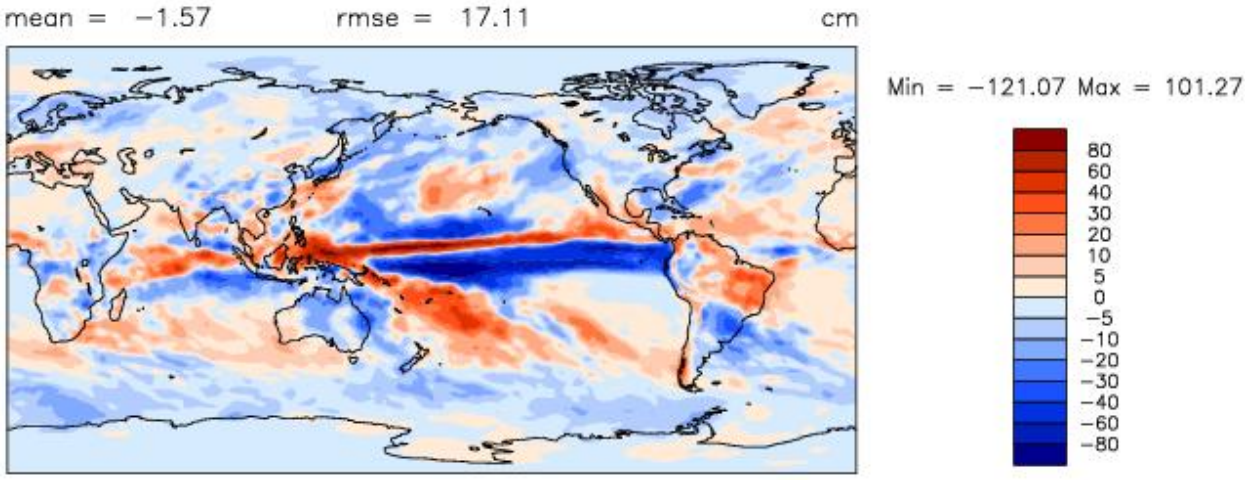

Figure 4.14. Annual average global precipitation changes. Emissions with sequestration minus *control*.

4.3 SSP1-2.6 Result Summary

Figure 4.15 shows a comparison between the sequestration effect on global patterns of temperature in precipitation (seen in Figures 4.13 and 4.14) to the IPCC (2013) RCP 2.6 and 8.5 predicted changes with continuing emissions. The locations of increased precipitation and temperature shown in the RCP figures is counteracted with sequestration according to these results. Australia is shown to get drier in the RCP scenarios, and only parts of that continent have preventative drying with sequestration. This may be due to noise or teleconnections not averaged out in this simulation that would be in an ensemble run. For the temperature, the Arctic is one of the most sensitive areas prone to warming and is also the strongest counteraction per these experiments.

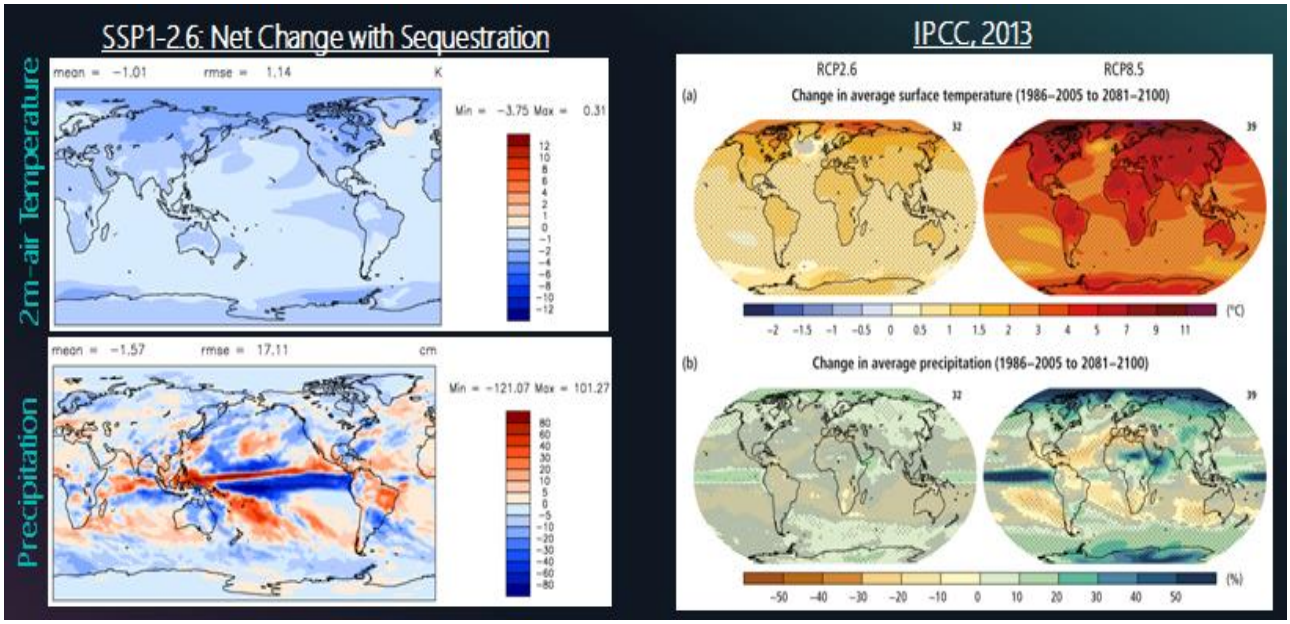

Figure 4.15. Experiments showing changes to global patterns due to sequestration throughout SSP1-2.6 compared to results from the IPCC (2013) RCP 2.6 and RCP 8.5 future outcomes.

A large ensemble of these simulations would bring a more well-rounded comparison to the RCP per the IPCC. However, the locations experiencing climate change counteraction in the sequestration experiment are the same locations showing significant effects of climate change in the IPCC results. This shows reliability in the model in producing similar results. From the results shown, the Arctic is one of the most sensitive locations to warming due to climate change, and is also the strongest responder to preventative climate change due to CDR. All locations experience ~1 K counteraction to climate change including oceanic regions. The polar regions had a decreasing trend in temperature throughout the sequestration simulation compared to the other latitudes that essentially maintained temperatures. The zonal wind did not experience much change due to sequestration except for in parts of the stratosphere due to prevention of cooling. These results show that CDR can more than abide to the Paris Agreement by preventing the 0.5-1 K of additional warming to the already warmed climate.

CHAPTER 5. SUMMARY, FUTURE CONSIDERATIONS, AND CONCLUSIONS

A initial study of the meteorological response to carbon dioxide sequestration and storage in Antarctica has been conducted using the CESM 2.1.1 model. Various sequestration scenarios were considered on various time scales. In a 15 year period, immediate drastic sequestration back to preindustrial levels along with industrialization showed a 0.5 K decrease in temperature while shutting off industrialization was less effective. For the SSP1-2.6 experiment, sequestering for 50 years prevented the 1^{o}C of warming by the mid-21st century. Areas showing strong counteraction of warming and precipitation due to sequestration are the same areas of strong warming and precipitation in the IPCC (2013) RCP scenarios.

As for the latitude response, the tropics and southern hemisphere middle latitudes had the weakest response in the short term simulations and the polar regions had the strongest signal. However, the SSP1-2.6 latitudinal response was relatively uniform for all latitudes with the polar regions having the strongest response to sequestration. Temperature and downward longwave radiation responded more to the increase in CO_2 throughout the 50 year simulation. Examination of methods employed, other feedbacks, and future considerations are discussed below.

5.1 Methods Discussion & Other Feedbacks to Consider

The model and data selection simulated a control average temperature of 288.04 K which is comparable to the 288.05 K global average temperature. The prognostic CO_2 cycle with the anthropogenic emissions showed a comparable trend to the CO_2 in the atmosphere with only a slight lag. While there is confidence in model performance, more data from various simulations would enforce that confidence. Ensemble runs would give the data range as demonstrated in the IPCC report and the GLENS program at NCAR. These types of runs would also distinguish the signal of sequestration more by averaging out the teleconnections that influence interannual variability.

Other feedbacks that were not the focus of this study that need to be considered in future work include the carbon cycle, land ice evolution, and sea level rise. The IPCC (2013) explained that models simulating CDR showed carbon dioxide outgassing from the ocean and land, but there is low confidence in the understanding of this result. When there is CO_2 depleted air

interacting with the ocean surface, there is a chemical reaction so that the ocean starts to outgas its own CO_2 (IPCC, 2013). The figures below show the surface CO_2 flux from the land (Figures 5.1 and 5.2) and ocean (Figures 5.3 and 5.4) for the control and sequestration. For the sequestration, the global annual average ocean carbon surface flux flips sign indicating outgassing after 15 years and 30 years for the land to start outgassing. The carbon uptake in the ocean for the control increases throughout the simulation and the land uptake maintains roughly the same amount.

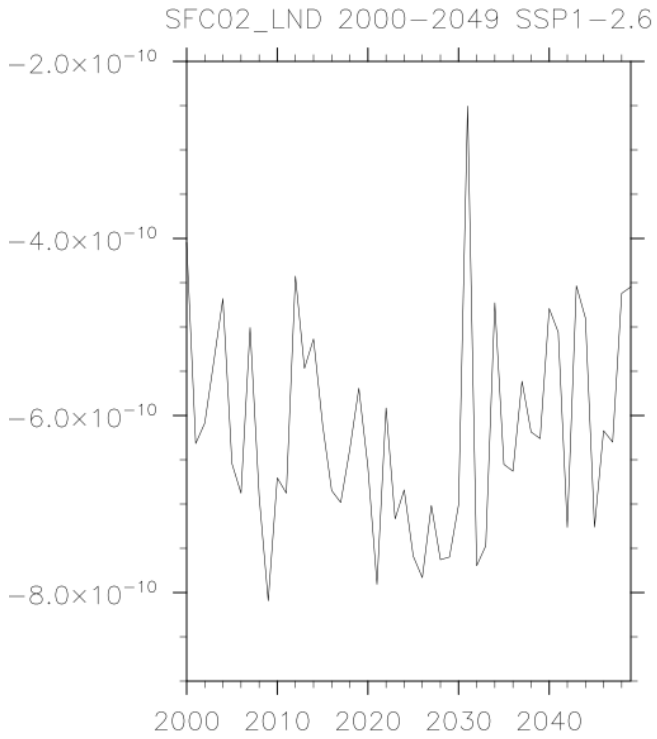

Figure 5.1. *Control* global annual average surface land CO_2 flux(kg/m^2/s)..

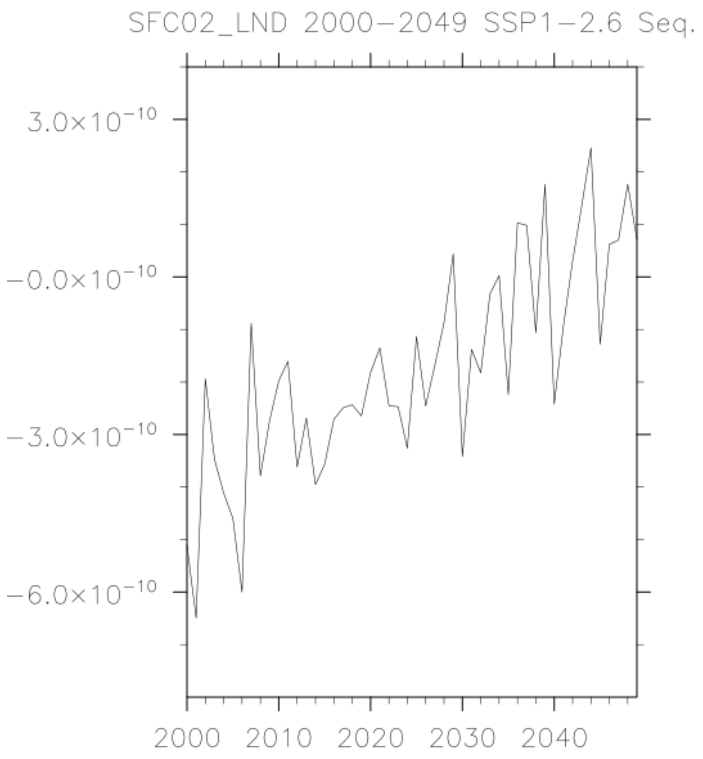

Figure 5.2. Sequestration global annual average land surface CO_2 flux(kg/m^2/s).

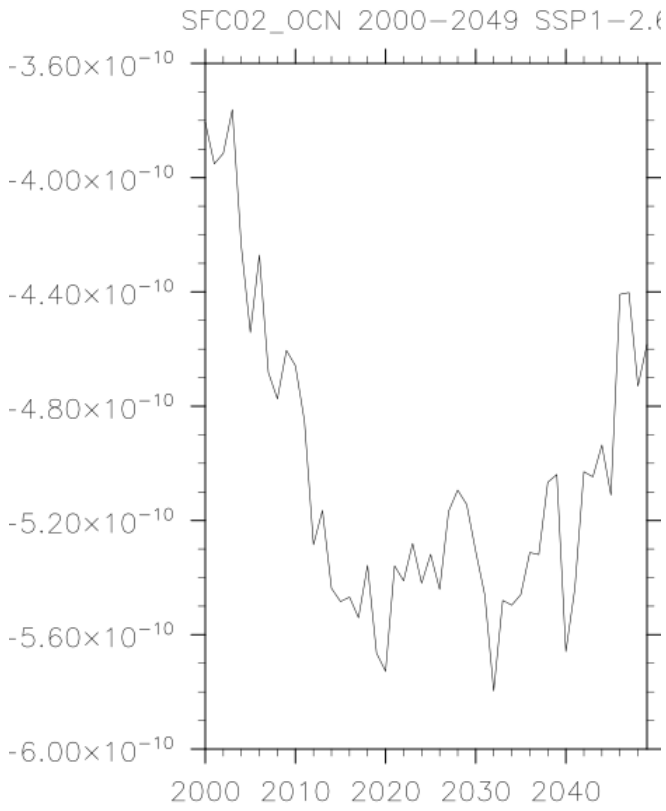

Figure 5.3. C*ontrol* global annual average ocean surface CO_2 flux(kg/m^2/s).

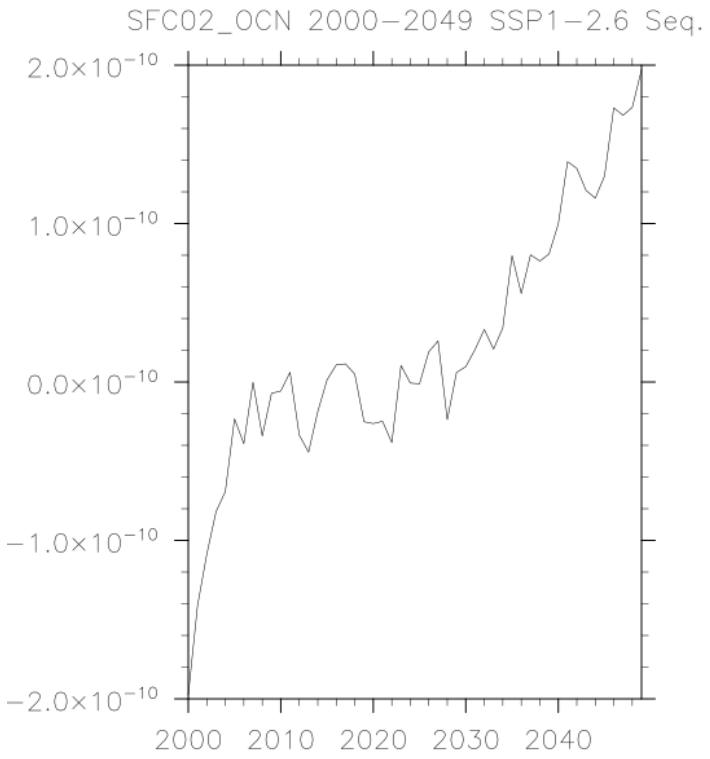

Figure 5.4. Sequestration global annual average ocean surface CO_2 flux ($kg/m^2/s$).

Land ice evolution was not considered in this study but would be an interesting addition to future simulations due to the sequestration being proposed in Antarctica. Land ice melt also contributes to sea level rise, and that is another important component to climate change not examined in this study. Further, a comprehensive study of the ocean internal heat response to sequestration would also deepen the understanding of this Earth feedback. The proposing of ensemble runs would help with these future examinations as well.

5.2 Conclusions & Future Considerations

The first study of meteorological response to CDR in Antarctica has been described in this study. Shutting off industrialization is not as effective as ambitious sequestration for temperature response. Sequestration in Antarctica while emissions continue increases the hemispheric CO_2 gradient. To fully examine the effect of Antarctica CDR, it would be ideal to examine this type of sequestration in allowable areas of the northern hemisphere to compare response by latitude, weather variables, and CO_2 concentration. Further, a complete pre-

industrial experiment for comparison to the sequestration experiments would enhance the understanding of global pattern changes in atmospheric response due to sequestration in Antarctica. A net radiative forcing calculation would also be helpful in line with IPCC (2013). Limitations of this study include a lack of ocean and land analysis. Ocean storage of CO_2 could help explain hysteresis (Held et al., 2010) in the results presented here, though that was not analyzed. Further, teleconnection influence on results was not analyzed and that furthers the cause for multiple member ensemble runs. In addition to multiple member ensemble runs, a method of assessing statistical significance is also warranted for examining the robustness of these results. This type of simulation methodology can also be applicable to different kinds of CDR (amine-swing and carbonates) by moving the location of CDR around Earth. While there have been studies done to examine CDR on various emission scenarios and comparing the effect of albedo modification and CDR, the same could be done with the way CDR is simulated in the present study.

The study presented here is a way to examine this CDR technology on CO_2 transport and meteorological response. Logically, the other SSPs with less sustainability will have more CO_2 sequestered to combat the effects of climate change. These are still studies worth conducting as the future is subject to change, and getting ahead of increasing emissions is a reasonable approach. Further, technology still needs to be developed for CDR to be able to obtain the efficiency this study assumes. Many albedo modification studies consider the RCP 8.5 scenario and the technology for aerosol injections is not at that ability either. Examining the Earth system response takes precedence before investing in the development of these technologies. Increasing emissions over the last century have modified the climate, so all precautions need to be taken when considering any modifications for reversal of these effects.

REFERENCES

Agee, E. and A. Orton, 2016: An Initial Laboratory Prototype Experiment for Sequestration of Atmospheric CO_2, *J. Appl. Met. & Clim*., **55**, 1763-1770.

_____, A. Orton, and J. Rogers, 2013: CO_2 snow deposition in Antarctica to curtail anthropogenic global warming, *J. Appl. Met. & Clim*., **52**, 281-288.

Andre, B., Kluzek, E., Sacks, W., User's Guide to version 5.0 of the Community Land Model (CLM). (https://escomp.github.io/ctsm-docs/versions/release-clm5.0/html/users_guide/index.html)

Boucher, O., Halloran, P.R., Burke, E.J., Doutriaux-Boucher, M., Jones, C.D., Lowe, J., Ringer, M.A., Robertson, E. and P Wu, 2012: Reversibility in an Earth System model in response to CO2 concentration changes, *Environ. Res. Lett.*, **7**, 024013.

Cao, L., and K. Caldeira, 2010: Atmospheric carbon dioxide removal: long term consequences and commitment, *Environ. Res. Lett.*, **5**, 024,011, doi:10.1088/1748-9326/5/2/024011.

Christiansen, B., A. Guldberg, A.W. Hansen, and L.P. Riishøjgaard, 1997: On the response of a three-dimensional general circulation model to imposed changes in the ozone distribution, *J. Geo. Res.*, **102**, 13051-13077.

Committee on Geoengineering Climate: Technical Evaluation and Discussion of Impacts; Board on Atmospheric Sciences and Climate; Ocean Studies Board; Division on Earth and Life Sciences; National Research Council, 2015: Climate Intervention: Carbon dioxide removal and reliable sequestration. The National Academies Press, 154pp.

Diallo, M., B. Legras, E. Ray, A. Engel, and J.A. Anel, 2017: Global redistribution of CO_2 in the upper troposphere and stratosphere, *Atmos. Chem. Phys*., **17**, 3861-3878.

Danabasoglu, G., Lamarque, J. -F., Bachmeister, J., Bailey, D. A., DuVivier, A. K., Edwards, J., Emmons, L. K., Fasullo, J., Garcia, R., Gettelman, A., Hannay, C., Holland, M. M., Large, W. G., Lawrence, D. M., Lenaerts, J. T. M., Lindsay, K., Lipscomb, W. H., Mills, M. J., Neale, R., Oleson, K. W., Otto-Bliesner, B., Phillips, A. S., Sacks, W., Tilmes, S., van Kampenhout, L., Vertenstein, M., Bertini, A., Dennis, J., Deser, C., Fischer, C., Fox-Kember, B., Kay, J. E., Kinnison, D., Kushner, P. J., Long, M. C., Mickelson, S., Moore, J. K., Nienhouse, E., Polvani, L., Rasch, P. J., Strand, W. G. The Community Earth System Model version 2 (CESM2). *Journal of Advances in Modeling Earth Systems*, **12** https://doi.org/10.1029/2019MS001916

Haywood, J. M., A. Jones, N. Bellouin, and D. Stephenson, 2013: Asymmetric forcing from stratospheric aerosols impacts Sahelian rainfall. *Nat. Climate Change*, **3**, 660–665, https://doi.org/10.1038/nclimate1857.

Held, I.M., M. Winton, K. Takahaski, T. Delworth, and F. Zeng, 2010: Probing the fast and slow components of global warming by returning abruptly to preindustrial forcing, *J. Clim*., **23**, 2418-2427.

IPCC, 2013: Climate Change—The Physical Science Basis. Contribution of Working Group I to the Fifth Assessment Report of the Intergovernmental Panel of Climate Change. Cambridge University Press, 2216 pp.

Jones, C.D., Ciais, P., Davis, S.J., Friedlingstein, P., Gasser, T. Peters, G.P., Rogelj, J., van Vuuren, D.P., Canadell, J.G., Cowie, A., Jackson, R.B., Jonas, M., Kriegeler, E., Littleton, E., Lowe, J.A., Milne, J., Shrestha, G., Smith, P., Torvanger, A., and A. Wiltshire, 2016: Simulating the Earth system response to negative emissions, *Environmental Research Letters*, **11**, 095012.

Jones, A. C., J. M. Haywood, N. Dunstone, K. Emanuel, M. K. Hawcroft, K. I. Hodges, and A. Jones, 2017: Impacts of hemispheric solar geoengineering on tropical cyclone frequency. *Nat. Commun.*, **8**, 1382, https://doi.org/10.1038/s41467-017-01606-0.

Keller, D. P., Feng, E. Y., and A. Oschlies, 2014: Potential climate engineering effectiveness and side effects during a high carbon dioxide-emission scenario, *Nat. Comm*., 5:3304|DOI: 10.1038/ncomms430.

Kiehl, J.T., and B.A. Boville, 1988: The radiative-dynamical response of stratospheric-tropospheric general circulation model to changes in ozone, *J. Atmos. Sci.*, **45**, 1798-1817.

Kramer, David, 2020: Negative carbon dioxide emissions. In *Phys. Today* **73 (1),** pp. 44–51. DOI: 10.1063/PT.3.4389.

Kravitz, B., D. G. MacMartin , M. J. Mills, J. H. Richter, S. Tilmes, J.-F. Lamarque, J. J. Tribbia, and F. Vitt, 2017: First simulations of designing stratospheric sulfate aerosol geoengineering to meet multiple simultaneous climate objectives. *J. Geophys. Res. Atmos.*, **122**, 12 616–12 634, https://doi.org/10.1002/2017JD027006.

MacDougall, A.H., 2013: Reversing climate warming by artificial atmospheric carbon-dioxide removal: can a Holocene-like climate be restored? *Geo. Res. Lett.*, **40**, 5480-5485.

Miyazaki, K., P.K. Patra, M. Takigawa, T. Iwasaki, and T. Nakazawa, 2008: Global-scale transport of carbon dioxide in the troposphere, *J. Geo. Res.*, **113**.

O'Neill, B. C., Tebaldi, C., van Vuuren, D. P., Eyring, V., Friedlingstein, P., Hurtt, G., Knutti, R., Kriegler, E., Lamarque, J.-F., Lowe, J., Meehl, G. A., Moss, R., Riahi, K., and Sanderson, B. M.: The Scenario Model Intercomparison Project (ScenarioMIP) for CMIP6, *Geosci. Model Dev.*, **9**, 3461–3482, https://doi.org/10.5194/gmd-9-3461-2016, 2016.

O'Neill, B.C., Kriegler, E., Ebi, K.L., Kemp-Benedict, E., Riahi, K., Rothman, D.S., van Ruijven, B.J., van Vuuren, D.P., Birkmann, J., Kok, K., Levy, M., Solecki, W., 2017. The roads ahead: Narratives for shared socioeconomic pathways describing world futures in the 21st century. *Glob. Environ. Change*, **42**, 169-180.

Smith, R., Jones, P., Briegleb, B., Bryan, F., Danabasoglu, G., Dennis, J., Dukowicz, J., Eden, C., Fox-Kemper, B., Gent, P., Hecht, M., Jayne, S., Jochum, M., Large, W., Lindsay, K., Maltrud, M., Norton, N., Peacock, S., Vertenstein, M., Yeager, S., The Parallel Ocean Program (POP) Reference Manual. (https://ncar.github.io/POP/doc/build/html/reference_manual/POPRefManual.html)

Tavoni, M. and R. Socolow, 2013: Modeling meets science and technology: an introduction to a special issue on negative emissions, *Clim. Change*, **118**, 1-14.

Tilmes, S., Sanderson, B. M., & O'Neill, B. C., 2016: Climate impacts of geoengineering in a delayed mitigation scenario. *Geophysical Research Letters*, **43**, 8222-8229. doi:10.1002/2016GL070122.

Tilmes, S., Richter, J. H., Kravitz, B., MacMartin, D. G., Mills, M. J., Simpson, I. R., … Ghosh, S., 2018: CESM1(WACCM) stratospheric aerosol geoengineering large ensemble project. *Bulletin Of The American Meteorological Society*, **99**, 2361-2371. doi:10.1175/BAMS- D-17-0267.1

Tokarska, K.B., and K. Zickfield, 2015: The effectiveness of net negative carbon dioxide emissions in reversing anthropogenic climate change, *Environmental Research Letters*, **10**, 094013.

Xu, X.Y., Lin, L., Tilmes, S., Dagon, K., Xia, L., Diao, C., Cheng, W., MacMartin, D., Wang, Z., Simpson, I., Burnell, L., 2020: Climate engineering to mitigate the projected 21st century terrestrial drying of the Americas: Carbon Capture vs. Sulfur Injection. *Earth System Dynamics*, https://doi.org/10.5194/esd-2020-2.

Zickfield, K., MacDougall, A.H., and Matthews, H.D., 2016: On the proportionality between global temperature change and cumulative CO_2 emissions during periods of net negative CO_2 emissions, *Environmental Research Letters*, **11**, 55006.